INVESTIGATION OF AGE RELATED CHANGES IN PORCINE CORTICAL BONE WITH A FOCUS ON THE REFERENCE POINT INDENTATION TECHNIQUE

BY

ALEXANDER SETTERS

THESIS

Submitted in partial fulfillment of the requirements
for the degree of Master of Science in Mechanical Engineering
in the Graduate College of the
University of Illinois at Urbana-Champaign, 2014

Urbana, Illinois

Adviser:

Professor Iwona Jasiuk

ABSTRACT

This thesis focuses on reference point indentation (RPI) as a method to determine age related changes in porcine cortical bone. RPI uses a reference probe that sets the zero position for a test probe, which indents samples over a number of cycles. Various polymers and porcine cortical bone have been utilized to further understanding of the RPI technique. The goal of this research is to use this novel equipment to determine differences in mechanical properties of bones, specifically young porcine bones. While RPI is the main technique used in this study, it has been supplemented by techniques such as scanning electron microscopy (SEM), three-point bend tests, nanoindentation, computed tomography (CT) scans, and bone material strength (BMS) measurements made using the Osteoprobe, a clinical indentation device. This thesis is comprised of three separate studies.

The first study in this thesis analyzes the RPI testing procedure using six month porcine cortical bone with the intent of developing a standard test procedure. The RPI outputs were analyzed as a function of force magnitude, preconditioning, variation within a sample and between samples, number of cycles, indentation surface (transverse versus longitudinal, polished versus unpolished), and micro-computed tomography radiation exposure. SEM was used as support for the choice of force magnitude.

The next study in this thesis is an investigation into the connection between RPI measurements, Osteoprobe measurements and known material properties of nine polymers. Eight 3D printed polymers and a standard polymer included with the RPI test machine were tested using

both RPI and the Osteoprobe. These results were then compared to each other as well as the polymers' known material properties.

The final part is the main study of this thesis. In this study, age related changes in porcine cortical bone were analyzed using RPI as well as several other experimental techniques. This study used porcine bones obtained from animals of 0 to 20 weeks of age at four week intervals, resulting in six separate age groups evenly spaced throughout the animal's early developmental stages. Tests used to determine the age related changes were three-point bend tests, nanoindentation, CT scans, RPI measurements and BMS measurements.

ACKNOWLEDGEMENTS

I want to extend my sincere gratitude to Professor Iwona Jasiuk for all of her assistance, guidance and support. I greatly appreciate all the time she dedicated to my studies and for all of her technical guidance, advice and encouragement. I would like to express my appreciation to Alexander Proctor, Davis Brimer, Peter Burks and all those at Active Life Scientific for their assistance with RPI and the Osteoprobe^{TM}. I would like to thank Kathy Walsh, Ted Limpoco and the MRL staff, and Scott Robinson for their equipment support and assistance. Many thanks to Dr. Steve Joslyn and those at VetMed for performing and analyzing the CT scans in Part 3. I would like to thank my collaborators within the Jasiuk research group for help with experiments and those in the Animal Science and Meat Science departments at the University for help with obtaining test material. Finally, I want to thank all my family and friends for their consistent support and inspiration throughout my education at the University of Illinois.

This research was supported in part by the National Science Foundation (NSF) grant CMMI 09-27909. Any opinions, findings, and conclusions or recommendations expressed in this material are those of the author(s) and do not necessarily reflect the views of the National Science Foundation. We also acknowledge the use of the Hysitron Triboidenter at the Materials Research Laboratory at the University of Illinois, which was purchased using the NSF grant MRI 09-23428.

TABLE OF CONTENTS

CHAPTER 1: GENERAL INTRODUCTION

Limited studies have been done on the mechanics of human bone for children. Obtaining young excised bones is very difficult and the opportunity to do so rarely presents itself. It is documented that porcine bone shows many similarities to human bone [1]. For this study, young porcine bones obtained through the Animal Sciences and Meat Sciences departments at the University of Illinois are used as a substitute for human bones. Animals from 0 to 20 weeks of age, at four week intervals, are analyzed using several techniques. The main technique used throughout this thesis is reference point indentation (RPI). This microindentation technique is performed through a device called BioDent (Active Life Scientific, Inc., Santa Barbara, CA). Throughout this thesis, BioDent measurements will be referred to as RPI measurements, since BioDent was the original RPI device. It is a relatively new device designed to measure bone properties *in vivo* [2, 3, 4]. It uses a reference probe, that rests on the sample surface, to set the zero point for measuring displacement with the test probe, which moves through the reference probe in a number of cycles to indent the sample [2]. The outputs from RPI are listed in Table1. Another microindentation device featured within this thesis is the Osteoprobe (Active Life Scientific, Inc., Santa Barbara, CA). While considered a reference point indentation device, the Osteoprobe makes a single impact indentation, rather than indenting over several cycles like the original RPI technique [5]. The Osteoprobe still measures a reference point before the impact indentation, hence the RPI classification. The other difference between RPI and the Osteoprobe, is the measured quantities. Instead of the nine parameters listed in Table 1, the Osteoprobe determines a parameter called bone material strength (BMS) [5]. Throughout this thesis, Osteoprobe measurements and BMS measurements will be used to describe tests run using the Osteoprobe device.

This thesis takes a multi-step approach towards determining age related changes in developing porcine bone. The first study is intended to determine the optimal method for using the RPI technique on porcine bones. Creating this method will allow data to be compared across studies in the future. After working towards standardization of the RPI technique, how this technique relates to other tests and traditional properties should be investigated. The second study covers this topic, using simplified polymeric materials to compare RPI outputs, BMS and known material properties. Using standard materials, correlations can be drawn without the heterogeneity of bone needing to be accounted for. The last part, which is the main focus of this thesis, takes findings from the first two studies into consideration when using RPI to determine age related changes. Bending tests, computed tomography (CT) scans, nanoindentation and BMS measurements are used to supplement the use of RPI as a tool to determine the age related changes. In summary, this thesis takes steps to investigate the age related changes in porcine cortical bones by focusing on how RPI can identify these changes.

CHAPTER 2: TOWARDS A STANDARDIZED REFERENCE POINT INDENTATION TESTING PROCEDURE[1]

Abstract

We study the reference point indentation (RPI) technique which has a potential to directly measure mechanical properties of bone in patients. More specifically, we tested 6 month swine femoral cortical bone at mid-diaphysis region to investigate the effect of several testing variables on the RPI outputs. They include the force magnitude, preconditioning, variation within a sample and between samples, number of cycles, indentation surface (transverse versus longitudinal, polished versus unpolished), and micro-computed tomography radiation exposure. The force magnitude variation test shows that all RPI parameters increase linearly with the increasing force magnitude except the indentation distance increase which shows a cubic trend with a constant force value between 4N and 8N. Preconditioning does not affect the trends for a force magnitude variation test. The cycle variation test shows that most RPI parameters reach either a maximum or minimum at 15-20 cycles. Transverse surface measurements are more consistent than the longitudinal surface measurements, but a rough surface and periosteum on the longitudinal surface could account for this difference. Exposure to the micro-computed tomography radiation in general does not have effect on the RPI measurements. [1]For the 6 month swine femoral cortical bone, testing using 6N force and 20 cycles with preconditioning on an unpolished longitudinal surface is recommended. This study advances our knowledge on how the RPI testing variables

[1] This part appeared in its entirety in the Journal of the Mechanical Behavior of Biomedical Materials.

Setters, A., Jasiuk, I., 2014. Towards a standardized reference point indentation testing procedure. Journal of the Mechanical Behavior of Biomedical Materials 34, 57-65.

influence the RPI outputs and provides guidance on the RPI measurements. It may also serve as a framework for developing a standardized testing procedure for the RPI technique.

2.1 Introduction

Reliable prediction of bone strength is an outstanding medical challenge. A novel microindentation technique, known as the reference point indentation (RPI) technique [2, 3, 4] has potential to directly measure cortical bone properties in patients [6, 7]. The RPI technique consists of a reference probe, which stays on the bone surface, and a test probe, which moves relative to the reference probe while indenting the bone (Figure 1). The RPI technique involves successive indentation cycles which create local damage in the bone. Published studies on the RPI technique have either compared the RPI outputs obtained by testing bone in different conditions (e.g. healthy versus diseased) or studied relationships between the RPI outputs and properties of cortical bone measured using traditional mechanical tests [3, 4, 6, 8, 9]. While comparing outputs does not necessitate a standard testing procedure, such a standard would be beneficial towards developing relations between the RPI outputs and mechanical properties of bone. This is due to the fact that various factors such as the force magnitude, preconditioning, number of cycles, variation within and between samples, indentation surface and radiation exposure can influence the RPI outputs. Thus, in this chapter we are investigating the effect of the above factors on the RPI outputs to provide guidance on the RPI testing. Our goal is to develop the framework for a standardized testing procedure for the RPI technique.

2.2 Materials

All samples were prepared from 6 month swine femurs provided by the Meat Sciences Department at the University of Illinois at Urbana-Champaign. Seven femurs from four different

animals were used for this study. One femur was used for each test except for the sample variation tests that used two femurs to compare the data obtained by testing cortical bone from two different animals. The femurs were wrapped in a phosphate-buffered saline (PBS) soaked gauze and stored frozen at -20°C until analysis. Bones were allowed to thaw for 24 hours at 4°C before sample preparation and testing. Samples were taken from the mid-diaphysis region of femurs. Each sample was divided into four quadrants: posterior, medial, anterior, and lateral. Transverse and longitudinal surfaces were prepared. The longitudinal surface is the outer surface of the bone and the transverse surface is the surface created by cutting the bone perpendicular to bone's long axis. The longitudinal surfaces were cleared from soft tissue and either polished or remained unpolished, depending on the test, while all transverse surfaces were polished. The polishing procedure involves a succession of finer grit sandpapers and polishing cloths and powders. The polishing stages were as follows: P180, P280, P400, P800, P1200, P2400, and P4000 sandpaper followed by micron cloth/powder combinations of 1µm/1µm, 0.25µm/0.3µm, and 0.25µm/0.05µm. Bone samples were kept wet during the RPI testing by placing a few drops of PBS on the bone surface just prior to the RPI testing. Additional, sample preparation details specific to each test are described in the Methods section. The BioDent™ Hfc reference point indentation instrument (Active Life Scientific, Inc., Santa Barbara, CA) was used for all microindentation tests.

2.3 Methods

2.3.1 Data analysis

For each comparison test the following RPI outputs were obtained: the first indentation distance (ID1), first creep indentation distance (CID1), first unloading slope (US1), total indentation distance (TID), indentation distance increase (IDI), average creep indentation distance (AvCID), average energy dissipated (AvED), average unloading slope (AvUS), and average

loading slope (AvLS). Definitions of these quantities are given in Table 1. Figures 1 and 2 provide graphical representations of the RPI parameters. With the exception of the preconditioning, radiation exposure and sample variation test, one-way analysis of variance (ANOVA) was used to determine if the RPI outputs were significantly different for the studied variable in each comparison test. A Tukey test was then used to determine which means were significant. A confidence level of 95% ($p<0.05$) was considered statistically significant. For the radiation exposure test, a two-parameter t-test with the same confidence level was used. The statistical analyses were performed using ORIGINPRO v9.0 statistical analysis and graphing software (OriginLab Corp., Northampton, MA).

2.3.2 Force variation

The effect of force magnitude on the RPI measurements was investigated using a 2.5 cm long section of the mid-diaphysis of a femur. The only factor varied was the indentation force. The force magnitudes included 2N, 4N, 6N, 8N, and 10N. The number of cycles was kept constant at ten cycles and the indentation frequency was 2 Hz. The surface that was indented was polished using the procedure described in Section 2. Indents were performed on the polished longitudinal surface in the anterior and medial quadrants. These quadrants were chosen due to the already smooth nature of these surfaces before polishing. Ten indents were made along the length of the sample for each force magnitude. The indents were spaced approximately 2 mm apart.

2.3.3 Scanning electron microscopy of force variation indents

Scanning electron microscopy (SEM) images of the indent sites were taken for the force variation test. All SEM images were done using a Philips XL30 ESEM-FEG. After testing, the sample was placed in a solution of 3% hydrogen peroxide for 24 hours to remove soft tissue. The

sample was then placed in a fixative solution (2.0% Formaldehyde, 2.5% Glutaraldehyde, 0.1M Na-Cacodylate [pH 7.4]) for 24 hours. Once the sample was fixed, the sample was placed in a buffer rinse of 0.1M Na-Cacodylate for 2 hours. Following the rinse, the sample was then dehydrated using the following series of ethanol rinses: 37% ethanol for 2 hours, 67% ethanol for 2 hours, 95% ethanol for 2 hours, and 100% ethanol for 6 hours (three 100% ethanol rinses for 2 hours each). Immediately after dehydration, the sample was placed in 100% hexamethyldisilazane (HDMS) for 6 hours for critical point drying. The sample was then removed from the HDMS and allowed to air dry for at least 12 hours. The sample was then sputter-coated with gold-palladium. Each indent was imaged using beam energy of 5.00 kV and spot size of 3.

2.3.4 Cycle variation

The effect of number of cycles was studied using again a 2.5 cm long section from the mid-diaphysis of a femur. We did five different tests with 2, 5, 10, 15, or 20 cycles while the force magnitude was held constant at 6N and the indentation frequency was 2 Hz for each test. The indents were performed on a polished longitudinal surface, again in the anterior and medial quadrants. We polished the bone surface for better visualization of indents by SEM. Ten indents were made along the length of the sample for each test. The indents were spaced approximately 2 mm apart.

2.3.5 Effect of preconditioning

The RPI technique has an option to apply a series of initial preconditioning indents to displace soft tissue to ensure that subsequent indents are done on the surface of cortical bone. In this test, a 2.5 cm long section from the mid-diaphysis of a femur was used. The sample was left unpolished. Testing was done on the longitudinal surface in the anterior and medial quadrants,

again due to a smooth nature of the surface without polishing. A force was varied using 2N, 4N, 6N, 8N, and 10N. The number of cycles was held constant at 20 cycles and the indentation frequency was 2 Hz. Ten indents were done for each force magnitude. Every even numbered indent was done without using preconditioning for a total of five indents. The other five odd-numbered indents were done using preconditioning. The parameters used for preconditioning were 2N, 5 cycles, and 2 Hz.

2.3.6 Longitudinal versus transverse surfaces

In this test, the transverse surface measurements, done on polished surface, were compared to the unpolished and polished longitudinal surface measurements. For these measurements, an indentation force of 6N was used with 10 cycles with an indentation frequency of 2 Hz. The unpolished longitudinal surface was measured first. The sample was then cut in half to expose the inner transverse surfaces and the transverse and longitudinal surfaces were polished and tested. On the longitudinal surface, both unpolished and polished, five rows of three indents were made in each quadrant. On the transverse surfaces, eight indents were made in each quadrant.

2.3.7 Effect of micro-CT radiation

A 2.5 cm section of the mid-diaphysis of a femur was used to study the effect of micro-computed tomography (micro-CT) radiation on the RPI measurements. The sample was cut in half to expose mating transverse surfaces which were then polished. In this test, the longitudinal surface was left unpolished. One half was left intact and was used as the "before radiation" sample. The other was cut into the four quadrants. Each quadrant was then imaged using the micro-CT to expose it to radiation and then indented using the RPI technique. The Xradia MicroXCT-200 was used to perform the scans. The micro-CT parameters used were 120 kV, 10W and a 10 second

exposure time with a total of 389 images per scan. Each scan lasted approximately 2 hours. This was the “after radiation” sample. Since micro-CT testing is done in dry conditions, each sample was allowed to dry for the same amount of time. Eight indents were done on the transverse and longitudinal surfaces for each quadrant. Each test used the indentation force magnitude of 6N, ten cycles, and indentation frequency of 2 Hz. Preconditioning was done on these samples using 2N over 5 cycles at 2 Hz.

2.3.8 Sample variation

Variations between two samples, taken from two different animals, and within a single sample were investigated in this test. The two 2.5 cm long samples were cut from the mid-diaphysis of two femurs from different animals. Three columns of nine indents were made along the length of the longitudinal surface of each sample for each quadrant. The samples were left unpolished so preconditioning was used. The parameters for preconditioning were 2N, five cycles and 2 Hz. For the test, 6N, 20 cycles, and 2 Hz were used.

2.4. Results

2.4.1 Force variation

The effects of force magnitude on the RPI measurements are shown in Fig. 1. With the exception of the IDI output, each RPI output shows a linear increase as the force magnitude increases, so linear fits were made for these outputs. Since the loading time is constant between tests, linearity could be a result of increasing the loading rate with increasing force. IDI shows a plateau in the measurements between 4N and 8N, so a cubic equation was used to fit to the data. One-way ANOVA tests indicated that there were significant differences within the IDI parameter at a 10N force magnitude. The results of the Tukey test for IDI are shown in Table 2. The force

magnitude of 10N shows significant differences ($p<0.05$) between all other forces. The force magnitudes of 2, 4, 6, and 8N show no significant differences ($p>0.05$) between themselves. SEM images of select indents are shown in Fig. 2.

2.4.2 Cycle variation

The effects of number of cycles on the RPI outputs are illustrated in Fig. 3. The outputs that exhibited adherence to a logarithmic function (IDI, AvCID, AvED and AvLS) are plotted with trend lines. All other outputs show little or no change as the number of cycles increases. The results of the one-way ANOVA tests indicate that each output shows significant differences. The Tukey test results summarizing these differences are presented in Table 3.

2.4.3 Effect of preconditioning

Figure 4 shows that the effect preconditioning has on the force variation is minimal. The only major difference is seen for the ID1 and TID parameters. The force magnitude variation still shows a linear increase for all parameters, except IDI, as indicated in the previous force magnitude tests. In this test, IDI shows a linear trend instead of the cubic trend seen in the previous test. The standard deviation did not consistently decrease for all tests.

2.4.4 Longitudinal versus transverse surfaces

The RPI outputs obtained by indenting polished transverse surfaces and polished and unpolished longitudinal surfaces are shown in Fig. 5. Each output, except US1, AvUS, and AvLS, obtained by testing the unpolished longitudinal surface has a higher value, whereas those obtained by testing the transverse surface and the polished longitudinal surface give similar lower values. Tukey tests showed that, for every output, there were statistically significant differences ($p<0.05$) between all surfaces and surface preparations. The only exception was for IDI and AvED, where

there was no significant difference ($p>0.05$) between the polished longitudinal and transverse surfaces.

2.4.5 Effect of micro-CT radiation

In this test, the RPI measurements were done to compare bone properties before and after the bone samples have been exposed to the micro-CT radiation. The test was done on both the longitudinal and transverse surfaces. Comparisons were made for each surface; results for the longitudinal and transverse surfaces were not compared to one another. Results from the t-tests showed that the only significant differences ($p<0.05$) present were for the US1, AvUS and AvLS for the transverse surface. No significant differences were observed for the longitudinal surface.

2.4.6 Sample variation

Effect of sample variation was studied by indenting along the length on the unpolished longitudinal surface for each quadrant. The data (not shown) for all outputs was closely grouped for each quadrant. There were differences between quadrants in both samples (mainly due to few outlier points in the lateral and posterior quadrants), but the difference between the two sample averages, combining results from all four quadrants, was not statistically significant.

2.5 Discussion

2.5.1 Force variation

Since only IDI exhibits nonlinear behavior, it will be the only RPI output measured to be discussed. The force magnitude will always affect all the other outputs. Thus, IDI and the analysis of the SEM images should be used to justify the choice of force magnitude for a given bone type. By examining the IDI outputs, one can see that 10N produces results that are significantly different than the results of the four other forces. All other forces produce IDI results that are statistically

similar. Since the IDI parameter has been shown to correlate with and predict toughness and energy to fracture obtained through traditional mechanical testing, it is recommended that 10N not be used due to the significantly different results it can produce [8]. This leaves only 2N through 8N as choices. SEM images of select indents (Fig. 4) support the elimination of the 2N force from consideration. The images show that the reference tip of the indenter moved, or "skipped," during testing. Since the machine was not disturbed during testing, the vibrations in the room could be one cause for this "skipping." This movement shows that the reference force for 2N is not sufficient to hold the reference probe on a smooth and hard material, such as the polished 6 month cortical bone that was used. This movement caused cycles beyond the first cycle to exhibit first cycle behavior, and affect the RPI results. The "skipping" causes other cycles beyond the first to penetrate an undamaged surface, resulting in more visible damage for a "skipped" indent than for a typical indent (Fig. 4). Since the remaining forces; 4N, 6N and 8N; are similar for the IDI output, any one of them would be suitable. 6N is a choice that reflects the average of all other parameters since the relationships are linear, so 6N is the recommended force magnitude. Note that in this test we used a polished surface so we could do SEM imaging. SEM images were not visible on unpolished longitudinal surfaces.

2.5.2 Cycle variation

In the discussion of this test we will focus on the four RPI parameters that show logarithmic behavior (IDI, AvCID, AvED, and Av LS) as a function of number of cycles. All other parameters have random variations that could be a result of the effect of the anatomical location or microstructure of the sample. AvCID and AvED decrease as the number of cycles increases. As the bone is compacted through repeated cycles, the amounts that the sample can creep and dissipate energy are decreased. By adding more cycles to the test, and decreasing the creep and energy

dissipated after each cycle, we see the reduction in the means of these quantities. These quantities seem to reach a minimum as the number of cycles increases. The opposite can be said of the IDI and AvLS outputs. As more cycles are added to the test, the material compresses and the increase in the indentation distance and the loading slope is reduced after each cycle. These values reach a maximum as the number of cycles increases. Based on these four parameters, we observe that 20 cycles would be the appropriate choice for testing.

2.5.3 Effect of preconditioning

The addition of preconditioning to testing does not have an effect on the trends except for ID1 and TID. The tests with preconditioning show lower values for these two outputs. This is due to the fact that the preconditioning portion of the test behaves like a normal indent and will have an indentation distance associated with it. Once the test is completed, the preconditioning data is discarded, thus resulting in a lower indentation distance for the ID1 and TID tests. Since the trends are more important than a constant shift in the data, we can say that preconditioning has no effect on the data. We also looked at the effect of preconditioning on standard deviation. By removing any variability that can arise due to soft tissue or periosteum, we expected the standard deviation to decrease. The data in Fig. 4 shows that the standard deviation, or scatter in data, does not always decrease. This could be due to the limited number of tests performed so more tests would be needed for a solid conclusion.

2.5.4 Longitudinal versus transverse surfaces

For these tests, more consideration is needed beyond determining which surface type (longitudinal vs. transverse) and preparation (polished vs. unpolished) provides minimal variation. If a bone were to be tested in vivo, the surface would not be polished and indentation on the

transverse surface would not be possible. When taking this fact into consideration, we can see that the unpolished longitudinal surface always presents significantly different data for all of the RPI outputs. Future studies would want to compare traditional tests to RPI measurements taken in vivo. Since the unpolished longitudinal surface would be closer to an in vivo test when compared to polished longitudinal and transverse surfaces, the appropriate surface to take future RPI measurements would be an unpolished longitudinal surface. This would allow correlations between traditional tests and RPI tests to be more readily applied to the in vivo RPI tests. However, the measurement on the transverse surfaces in a research setting can provide additional insights on bone, in particular on its anisotropy.

2.5.5 Effect of micro-CT radiation

The purpose of this test was to determine if the radiation from micro-CT imaging affects the RPI outputs. Hansma et al. had shown that radiation can adversely affect RPI parameters [3]. This test was conducted to ensure that radiation from micro-CT imaging did not have adverse effects on the RPI parameters. This would allow imaging to be done before and after testing to see the microstructure that was indented upon. Significant differences ($p<0.05$) between the before and after exposure samples were observed for the US1, AvUS and AvLS parameters for the transverse surface. No significant differences ($p>0.05$) were observed for the longitudinal surface. Because *in vivo* testing is done on the longitudinal surface, micro-CT can be done before RPI tests that are being used to approximate *in vivo*. Since only IDI and AvED have been shown to correlate to traditional mechanical properties, the differences on the transverse surface are not as important. Due to this, we conclude that the radiation from micro-CT does not adversely affect the important RPI parameters.

2.5.6 Sample variation

With the exception of some outlier data, the measurements made along the length of the samples are very consistent. The major outliers in the lateral and posterior quadrants can be explained by the heterogeneity of bone's microstructure. There could have been resorption cavities under the surface of the bone where these outlier indents took place that would explain the larger than average RPI outputs. There is also some scatter towards the end of the lateral quadrant. This location has soft tissue insertion sites present which give a rough surface as well as make it difficult to remove all soft tissues from the sample. These insertion sites can easily account for this scatter at the end of the sample. We find that the RPI measurements are consistent along the length of the sample. Thus, the local measurements at the middle of the sample are representative for a studied length of 2.5 cm in the mid-diaphysis region.

2.6 Summary

We recommend that for a 6 month porcine femoral bone the RPI testing is done on an unpolished longitudinal surface using 6N force and 20 cycles. We find that preconditioning has a small effect on the RPI results aside from decreasing the ID1 and TID data without affecting the trends. We found relatively small variation in the RPI outputs within and between samples. The effect of radiation is not significant on the longitudinal surface and does not affect any important parameters on the transverse surface. While this work provides further insights on the RPI technique, it has several limitations. We only investigated 6 month swine femurs. Further studies would require varying ages, species, and bone types. In each test we only used one femur, with the exception of the sample variation test, where two femurs were used, since multiple indents could be made on a single sample. Further studies involving larger number of samples and additional testing parameters could be done to provide additional data.

2.7 Acknowledgements

This research was supported by the National Science Foundation (CMMI 09-27909) (I.J.).

The authors declare no conflict of interest.

CHAPTER 3: CORRELATIONS BETWEEN REFERENCE POINT INDENTATION AND MATERIAL PROPERTIES OF POLYMERIC MATERIALS

Abstract

Correlations between reference point indentation (RPI), Osteoprobe measurements and traditional material properties are investigated. The investigation is simplified by testing stiff isotropic polymers instead of anisotropic bone, the material that RPI and the Osteoprobe were indented to be used on. Nine different polymers are used. One was included with the RPI machine and the other eight are 3D printed polymers. Tensile modulus and strength, flexural modulus and strength, elongation at break and Izod impact energy were obtained through material data sheets or online resources and plotted against the nine RPI outputs and BMS obtained though the Osteoprobe. RPI measurements were also analyzed against BMS data. ID1 and TID showed strong correlation to BMS. ID1, TID, US1, AvUS and AvLS, as well as BMS, show the best correlation to Izod impact energy. Elastic and flexural moduli show moderate correlations to the same RPI parameters and BMS. AvCID is the only RPI output to show correlation with elongation at break. Other material properties, such as tensile and flexural strength, show little to no correlation to RPI or Osteoprobe tests. This study aims to further the understanding of the RPI and Osteoprobe techniques by using simple materials and determining correlations. This study also serves to further the fundamental understanding of RPI and the Osteoprobe.

3.1 Introduction

Reference point indentation (RPI) is a relatively new technique that has been developed to measure the mechanical properties of bones *in vivo* [2, 3, 4, 6, 7, 9]. Currently, this device is only being used in a research setting. This technique uses a two-piece probe: an outer reference probe

that rests on the sample surface and provides the zero location for distance and an inner probe that is oscillated to indent the sample surface over several cycles [2, 3]. Examples of an RPI test and a typical RPI load-deformation curve can be seen in Fig. 1 and Fig. 2 respectively. This technique has seen increased use on bone in a research setting [3, 4, 6, 7, 8, 9, 10, 11, 12]. Since bone is a hierarchical and anisotropic material, results can vary based on various conditions [10]. However, only one study has attempted to standardize RPI tests [10] and there has only been one published work that used simpler materials (elastomers) to try and understand the RPI technique more fundamentally [13]. Another device, the Osteoprobe (Active Life Scientific Inc., Santa Barbara, CA, USA), has been created with the intent of having the device used clinically [5]. While the Osteoprobe is considered an RPI device, it performs its measurements using a single impact indentation rather than several indentations over a number of cycles [5]. It has been used in clinical research to measure a parameter known as Bone Material Strength (BMS) which is larger for healthier bones or stronger materials [14, 15, 16]. In this article, the authors attempt to show correlations between traditional mechanical properties, RPI measurements and Osteoprobe measurements using stiff 3D printed polymeric materials. The goal is to show whether mechanical properties are correlated the two RPI techniques and whether the RPI and Osteoprobe measurements can be used interchangeably as well. This study can also serve as a beginning to a more fundamental understanding of the RPI technique and the Osteoprobe.

3.2 Materials

Nine different polymers with varying material properties were used in this study. Eight of the polymers were 3D printed at the Ford Lab at the University of Illinois. These eight materials were ABS-M30 (ABS), polycarbonate-ABS (PC-ABS) and polycarbonate (PC) from Stratasys; FullCure720 (FC720) and VeroWhite (VW) from Objet; ProtoGen^{TM} O-XT 18420 (PG) and

WaterClear® Ultra 10122 (WCU) from DSM Somos and PA2200 Balance 1.0 (PA) from EOS GmbH. The last of the nine polymers was poly (methyl methacrylate) (PMMA) that was included with the RPI testing machine. The material properties used for analysis are given in Table 4. Values for the 3D printed materials were obtained from material data sheets included with the materials. If a range of values were given, the average was taken as the property value. For PMMA, values were taken online from eFunda [17].

3.3 Methods

For both RPI and Osteoprobe measurements, 5 indents were made per material. RPI measurements were made using a 6N force magnitude, 20 cycles and an indentation rate of 2Hz, according to recommendations from [10]. No preconditioning was necessary since these are not biological materials. Osteoprobe measurements were made by securing the samples to a heavy metal base and compressing the device over 1 second until the impact indentation was made. Three types of comparisons were made: RPI versus material properties, Osteoprobe versus material properties and RPI versus Osteoprobe. In each of these, Pearson's r values, a measure of linear dependence between two variables, are calculated to determine the strength of the correlation between different properties or outputs. Statistical significance was determined using a two-tailed test of significance. Statistics were analyzed using ORIGINPRO v9.0 statistical analysis and graphing software (OriginLab Corp., Northampton, MA). R^2 values, the square of the Pearson's r values, are included on plots of the data sets along with linear trend lines.

3.4 Results

3.4.1 RPI versus material properties

Each one of the nine RPI outputs (Table 1) has been plotted against several mechanical properties in Figs. 8-13. For flexural strength and Izod notched impact, there are no values reported on the data sheet for PA, so all data comes from the remaining eight polymers. Pearson's r values are reported in Table 5. Tensile strength does not show strong or moderate correlation with any of the RPI outputs, although all are statistically significant aside from IDI, AvED and AvLS. Elastic modulus shows high r values with statistical significance ($|r| > 0.64$) for all but CID1, IDI and AvCID. AvCID versus elongation at break has a statistically significant r value of 0.732, while all other parameters show very low correlation with no significance. Similar to tensile strength, flexural strength does not have any strong or moderate correlations to the RPI outputs and the same outputs show significance. Flexural modulus shows very low correlations and none are significant. Izod impact shows moderately strong correlations with ID1 and TID with r values at or above 0.8. US1 and AvUS show moderate correlations with Izod impact ($|r| > 0.7$) and the remaining RPI outputs show low or no correlation. The only correlations to Izod impact that are not significant are IDI, AvCID and AvED.

3.4.2 Osteoprobe versus material properties

Mechanical properties are shown plotted against BMS in Fig. 14. Trend lines and R^2 values are shown on each plot. Table 5 shows the Pearson's r values for each mechanical property versus BMS. Every property shows r values below 0.5 except for elastic modulus and Izod impact, which show r values of 0.781 and -0.855 respectively. Elongation at break and flexural modulus are the only non-significant correlations.

3.4.3 RPI versus Osteoprobe

The nine RPI outputs are plotted against BMS in Fig. 15. For this data, R^2 values with our statistical analysis are used since there is no way correlate a specific RPI measurement to an Osteoprobe measurement. Trend lines and R^2 values are again shown on each plot. ID1 and TID show very strong correlations with BMS. ID1 and TID both have R^2 values over 0.9. US1, AvUS and AvLS show moderately strong correlations with R^2 values over 0.63. AvED shows a moderate correlation to BMS with an R^2 value of 0.4502 and all remaining RPI outputs show little to no correlation.

3.5 Discussion

3.5.1 RPI versus material properties

It is easy to see that no strong correlations should exist between the RPI parameters and the tensile and flexural strengths. Both strengths refer to the limit of engineering stress in the material which is usually found through low loading rate mechanical tests on a large scale. Even though the material is plastically deformed through RPI measurements, the indentations are made on a small scale and at a high loading rate. Because polymers are viscoelastic, this change in scale and loading rate affects the outcome and results in the absence of correlation between RPI and strength.

Elastic modulus shows moderate correlations with US1, AvUS and AvLS. Since these three RPI outputs are slopes in the load deformation curve and the elastic modulus is the slope of the elastic portion of the stress-strain curve for a material, it makes sense that we see a reasonable correlation between the two. Since there is damage and deformation involved, the correlations are not expected to be perfect. The ID1 and TID parameters also show moderate correlation. The

higher the elastic modulus, the more resistant the material is to deformation, and we see this in the moderate correlation. As modulus increases, both ID1 and TID decrease. The same argument can be made for the moderate correlation with AvED. The more resistant a stiff material is to deformation, the less energy the material will dissipate as it is deformed. Thus, we see a decrease in AvED as modulus increases.

Flexural modulus, shows very small correlations, of which none are significant, with the RPI parameters. This can be partially explained by the loading direction. In a tensile, or compression, test the load is applied perpendicular to the long axis of the sample. In flexure, the sample is subjected to compression on the portion above the beam's horizontal axis and tension in the portion below. There is also shear involved. Since there is a variety of loading in flexure, we see slightly lower moderate correlations for the RPI slopes. Since RPI indentation distances resemble strains in compression tests, the remaining outputs do not show correlation. Measurement of strain in flexure depends on the curvature of the deflection, which does not occur in a compression test.

Of all the RPI outputs, we expect CID1, AvCID or both to have a correlation to elongation at break. In this case, only AvCID shows a moderate correlation that is significant. CID1 does not show a strong correlation because the sample is initially impacted and deformed on the first cycle and the extent of deformation on this first cycle can influence the amount that the sample will creep as the load is held. Once the material is compacted through successive indents, the average creep distance becomes a more consistent value characteristic of the material being tested. Thus, we see the strong correlation for AvCID and the very low correlation with CID.

The last property compared to RPI is Izod impact energy. We expect to see strong correlations with a few RPI outputs since the technique involves a series of impact indentations.

There are moderately strong correlations between Izod and ID1 and TID. ID1 shows the stronger correlation since it is the first indent and impacts undamaged material. Since TID is simply ID1 combined with the remaining cycles' indentation distance, which is small compared to ID1, we expect and get a correlation. This correlation is weaker than ID1, due to the variability in the remaining indentation distance. The correlation between Izod and US1 and AvUS can be explained in a similar manner as for elastic modulus and AvED. A lower stiffness, or unloading slope, results in a higher impact energy. The correlation between Izod and US1 and AvUS is moderate, but we do see this trend. We expected a correlation to AvED, but the scale to which the test occurs could have a large effect.

Tang et al. showed that testing elastomers using a tissue indentation device (TID) resulted in good correlations with other traditional measures [13]. The TID uses a flat cylindrical punch tip rather than the 90° cone of the RPI technique making more suitable to testing soft materials, which RPI cannot test. The TID also tests creep, stress relaxation and cyclic loading (without a creep hold segment), which is also different from RPI. Despite these differences, if correlations can be determined from TID, one would expect to determine correlations for RPI as well. We did find some correlations, but they were not exact. In experiments performed by Tang et al., materials were tested get the material properties rather than taking values from material data sheets, which could result in better correlations. Future work could involve creating samples to test ourselves, rather than relying on manufacturer data.

3.5.2 Osteoprobe versus material properties

The only moderately strong correlations between Osteoprobe measurements and mechanical properties were for elastic modulus and Izod impact energy. The large Izod correlation can be explained by the fact that Osteoprobe indents are essentially impacts, so the parallels are

clear. The differences can be explained by differences in scale and test setup. The correlation between elastic modulus and BMS can be explained similar to correlations seen between RPI parameters and elastic modulus. As the modulus increases, its resistance to deflection increases as well. This increase in resistance results in lower indentation distances in RPI tests. Since BMS is inversely proportional to the indentation distance [5] we see an increase in BMS as elastic modulus increases. The differences between a standard tensile test and the Osteoprobe impact tests, such as scale and loading rate, can help account for the difference.

3.5.3 RPI versus Osteoprobe

The RPI technique and the Osteoprobe are intended to measure similar properties. Both aim to determine a bone's susceptibility to fracture. While differences exist, such as impact loading for the Osteoprobe versus load-hold-unload style loading for RPI, each indent in RPI is essentially an impact so correlations should exist between the two techniques. Both techniques also make indentations on the micro-scale. We indeed see strong correlations as ID1 and TID both show R^2 values greater than 0.9. The BMS measure from the Osteoprobe is inversely related to the indentation distance from the impact onto the undamaged material. Both ID1 and TID contain indentation distances from an impacts onto undamaged material. TID is simply ID1 plus some other, much smaller distance value. Thus, we see an inverse correlation between BMS and the RPI values for ID1 and TID. As mentioned in previous sections within this discussion, the elastic modulus, related to the unloading slope, and impact energy, related to energy dissipated show inverse correlations with indentation distances. It is because of this that we see moderate to moderately strong correlations between BMS and US1, AvUS, AvLS and AvED.

3.6 Summary

There are several correlations that exist for the three different comparisons that we made. The strongest correlations were between RPI and Osteoprobe tests, simply due to the similar nature of the tests. ID1 and TID both show strong inverse correlations to BMS. Several other RPI outputs show moderate to moderately strong correlation to BMS. When it comes to traditional material properties, Izod impact energy shows the strongest correlations. RPI and Osteoprobe tests are micro-scale impact tests, so correlations are expected. ID1, TID and the loading and unloading slope outputs, as well as BMS, show the best correlation to Izod impact energy. Elastic and flexural moduli show moderate correlations to the same RPI parameters and BMS. AvCID is the only RPI output to show correlation with elongation at break. Other material properties, such as tensile and flexural strength, show little to no correlation to RPI or Osteoprobe tests. There are limitations to this study however. The nine materials used in this study had certain material properties that were within small range. For example, all the materials had elastic moduli between 1.5-3 GPa, which is a relatively small range. Future work could involve materials within a larger range of values for each material property. In addition, the material properties used in this study were limited to what was available on the material data sheets. Additional studies could generate or obtain other material properties such as fracture or bending toughness. Also, the material data sheet values listed were ranges so average values of these ranges were used. Future work could involve creation of samples to test properties of the polymers ourselves, rather than relying on material data sheet information. Simulations could also be done using these simplified materials to determine what material properties contribute the most to specific RPI outputs or BMS.

CHAPTER 4: EARLY DEVELOPMENTAL STAGE RELATED CHANGES IN MECHANICAL PROPERTIES OF PORCINE CORTICAL BONE

Abstract

This work focuses on analyzing several bone analysis techniques. Reference point indentation, the Osteoprobe, three-point bending tests, mineral content through CT scans and nanoindentation are used to determine any age related changes in developing porcine bone. These techniques are also compared against one another to determine if one test can be used in place of another. This is more relevant when attempting to validate a clinical device, like the Osteoprobe. Linking the bone mineral strength (BMS) measurements to a traditional test like three-point bending would provide quick and easy determination of traditional mechanical properties *in vivo*. RPI showed conflicting results among the three forces tested and different genetic lines gave different trends as a function of age. Three-point bend tests showed trends and significant differences ($p<0.05$) for flexural modulus and strain at break, but 0 week samples did not follow the trend and exhibited behavior similar to 20 week bone. Mineral content determined through CT scans did not show any trends or correlations as it was relatively constant across all ages. Nanoindentation indicated that 0 week bones could have a stiffer outer shell that gives them extra support that could explain differences in other tests, but more tests and information is needed before a strong conclusion can be drawn. Lastly, BMS measured through the Osteoprobe showed moderately strong correlation with age and Tukey tests showed that each age was statistically different ($p<0.05$) from one another, except for 16 versus 20 weeks. More tests and samples are needed, but overall, this work provides a firm background to develop more research in the area of young developing bone.

4.1 Introduction

Understanding the mechanical changes associated with bone development is still an outstanding challenge. While research has been done on aging bone in adults, healthy young human tissue is not a readily available resource for experimental research. Most research on young human bone tissue involves characterization of the effects disease has on bone. Berteau et al. has analyzed the elastic moduli of children's bones using ultrasound, but this method is non-destructive and the information that can be gained from such a test is limited [18]. The study also focused on a specific age range of children and compared them to adult bones. Rasoulian et al. have investigated young porcine bones, however only two age groups younger than six months of age were investigated [9].

One of the main techniques used in this work is reference point indentation (RPI). The technique has the capability of measuring properties of bones *in vivo* [2]. The technique uses a reference probe that rests on the sample surface and a test probe that is housed within the reference probe and indents the sample [2]. A schematic of this test can be seen in Fig. 1 and an example of a load-deformation curve for the technique is shown in Fig. 2. RPI has been correlated to toughness and has been used to successfully observe differences between healthy and diseased bone states [3, 4, 6, 7, 8, 11, 12]. Rasoulian et al. have used RPI to specifically investigate age related changes [9]. However, as mentioned earlier, ages younger than six months were limited to two age groups. The RPI technique has been used for *in vivo* work, which would make it a viable candidate to evaluate younger bone properties *in vivo* [6, 7]. This provides a unique ability to analyze the RPI technique as a candidate for *in vivo* measurement of the properties in young children. The same can be said of the non-reference probe version, the Osteoprobe [14]. This device has been used in a clinical setting and has been specifically designed for such tests [14, 15, 16]. The Osteoprobe

has not been used on young bones as well. Whether or not RPI and Osteoprobe measurements detect differences for such young bones is an outstanding issue. Bending tests, dynamic and static nanoindentation tests and computed tomography (CT) scans were used to supplement the RPI and Osteoprobe measurements. In this study, porcine tibiae ranging from 0 – 20 weeks of age, at 4 week intervals, are analyzed using the mechanical and imaging methods mentioned above. The goal of this work is to determine the differences in the mechanical response of early developing bone as a function of age and connect measurements made on these ages amongst the tests performed.

4.2 Materials

Porcine tibiae from six different age groups were obtained through assistance from the Animal Science and Meat Science Departments at the University of Illinois. Four genetic lines were obtained for this study and animals from each line are considered genetically similar since they were born from the same mother. These pigs were fed based on a phase-feeding program typical for the US swine industry, using diets based on corn and soybean meal with nutrient levels that meet or exceed recommendations set forth by the swine NRC (2012). Animals were harvested at 4 week intervals to give the following age groups: 0, 4, 8, 12, 16 and 20 weeks. Three of the 4 lines were complete. One animal died prematurely in the fourth line, so no 20 week sample is available for that line. Because of this, only bones from the three complete lines were used for this study. After harvesting, the bones were wrapped in gauze soaked in a phosphate buffered saline (PBS) solution and stored in a freezer at -20°C. Before use, bones were thawed for at least 24 hours at 4°C. Bones and bone samples were kept moist with additional PBS through all tests. The left tibiae from these lines were used for the RPI measurements, Osteoprobe measurements and CT scans. The right tibiae were used for bending test samples as well as for nanoindentation tests.

4.3 Methods

4.3.1 Reference point indentation

Whole tibiae were used for all RPI tests. Indentation forces of 6N, 8N and 10N were used. Measurements were done using 20 cycles and 2 cycles per second. Five indents were made on the flat anterior-medial surface of the tibiae. Tibiae were kept moist with applications of PBS before testing. Table 1 lists the outputs collected from the RPI tests.

4.3.2 Osteoprobe measurements

The same tibiae used for RPI were used for Osteoprobe measurements. Five indentations were made on the anterior-medial surface of the tibiae. Bones were kept moist with PBS before testing. In order to test with the Osteoprobe, the handheld device is compressed over 1 second until the device performs the impact indent [14]. The only parameter collected from the Osteoprobe is bone material strength (BMS) [14].

4.3.3 Three-point bend tests

Three-point bending tests were performed using small samples according to work done by Albert et al. [19]. Samples were cut from the anterior-medial portion right tibiae of one complete genetic line. Samples were cut using an IsoMet 1000 Precision Saw (Buehler, Lake Bluff, IL, USA) to dimensions of approximately 1mm x 0.5 mm x 5mm. Samples were prepared to be tested in the longitudinal direction as described by Albert et al. [19]. Tests were run using an MTS Insight Elecromechanical Uniaxial Testing Machine (MTS Systems, Eden Prairie, MN, USA). Samples were preloaded five times with a crosshead speed of 0.3mm/min to loads ranging between 0.05 –

1N [19]. After preloading, samples were then loaded until failure at a loading rate of 2mm/min. Load-deformation data was later converted to stress-strain data and the following parameters were calculated: flexural strength, flexural modulus, flexural strength and strain at break. Due to the difference in size of the tibiae, the number of samples from each age is not equal. The samples numbers are 2, 4, 5, 4, 9 and 9 samples for 0, 4, 8, 12, 16 and 20 weeks respectively.

4.3.4 CT scans

CT scans were obtained by an equipment expert at the College of Veterinary Medicine at the University of Illinois and scans were analyzed by Dr. Stephen Joslyn. All scans were performed using a helical multi-slice CT scanner (Lightspeed 16 slice, General Electric Medical Systems, Milwaukee, WI) and the following imaging parameters: 120 kVp, 120 mAs, 0.625 mm slice thickness and a pitch of 0.9375.

For all data sets for each specimen, the external soft tissues were removed via threshold segmentation using a dedicated DICOM workstation (OsiriX version 5.8.4 64-bit, OsiriX Imaging Software, OsiriX Foundation, Geneva, Switzerland) and segmentation plug-in (Mialite, Center for Medical Image Science and Visualization (CMIV), Linköping University, Sweden). A 3-dimensional maximum intensity projection reconstruction was used to remove all bone tissue except for the tibia. Segmentation of the external soft tissues required a Hounsfield unit (HU) threshold range of -500HU to 100HU, with a smoothing factor of 0.5 and a seed (starting point) within the external soft tissues [20]. The cortical and cancellous bone prevented the segmentation process from entering the medullary cavity of the bone. The full dataset of the segmented tibia was loaded into a separate image analysis program (Mango version 3.1.2, Research Imaging Institute, University of Texas Health Science Center, USA) to calculate the mean cortical bone density (Ct.HU). The Ct.HU was generated using a region of interest of 500HU to 3000HU and presented

HU. The mean cortical bone density was converted to mineral density using two published techniques [21, 22]. The first was established by Schileo et al. with the equation: ρ_{QCT} (mineral density) = (0.7764*HU)-5.6148 and ρ_{QCT} expressed as mg/cm^3 [21]. The second was established by Crookshank et al. with the equation: ρ_{QCT} = (HU – 22.806)/1.333 and ρ_{QCT} also expressed as mg/cm^3 [22].

4.3.5 Dynamic and static nanoindentation

Dynamic nanoindentation tests were performed using DMA III software on a TI 950 Triboindenter (Hysitron Corp., Minneapolis, MN, USA). Testing was carried out in part in the Frederick Seitz Materials Research Laboratory Central Research Facilities, University of Illinois. Samples were cut using an IsoMet 1000 Precision Saw from one right tibiae from the following age groups: 0, 8, 20 weeks. Samples were slices cut perpendicular to the long axis of the bone. Samples were submerged in PBS for testing and a fluid-cell Berkovich tip was used to perform the indentations. Samples were loaded to 3000μN over five seconds, subjected to a frequency sweep and then unloaded over five seconds. The frequency sweep kept the quasi-static load at 3000μN while oscillating at a load amplitude such that the displacement amplitude was approximately 1 and 2nm. Frequencies of 10-200 Hz, at 10 Hz intervals, were tested. Indentations were made starting at the surface of the anterior-medial and moving inwards towards the center of the sample to a depth of 200μm at 10 μm intervals. This was done to determine if the properties of the bone change as a function of depth into the bone. The depth was chosen to be 200μm since RPI indentations rarely go beyond that depth into the bone tissue. Three lines of indents were made per sample, resulting in 63 total indents per sample. The tan (δ) was recorded as it is considered a reliable measure of the viscous damping in a material [23]. Reduced elastic modulus and hardness were also calculated from the unloading portion of each test.

4.3.6 Statistical analysis

All statistical analysis was performed using ORIGINPRO v9.0 statistical analysis and graphing software (OriginLab Corp., Northampton, MA). One-way analysis of variance (ANOVA) was performed for all RPI tests, Osteoprobe measurements, three-point bending tests and CT scan mineral density measurements. Tukey tests were used to determine significant differences. Additional considerations may needed to account for the varying sample numbers in the bending tests. Correlation analysis (Pearson's r) was performed between age and the following: RPI outputs, BMS, bending test properties and CT scan mineral density. Pearson's r values were also determined for all possible combinations of correlations between RPI, BMS, bending properties and mineral density. Due to the limited number of samples, dynamic nanoindentation is only used for qualitative analysis and no statistics were done.

4.4 Results

4.4.1 Reference point indentation

The RPI outputs for each force measured (6N, 8N, and 10N) are plotted against age in Figs. 16-18. Tukey test results for the forces are shown in Tables 6-8. Table 9 shows the results of the age-RPI correlation analysis. For a 6N force, 8 weeks samples seem to be the most significantly different ($p<0.05$) from all other ages for most RPI parameters. There are also other random differences shown in Table 6. For 8N, 16 and 20 week samples are the ages that stand out in terms of significance. For most of the RPI parameters for 8N, they are statistically different ($p<0.05$) from all other ages. The 16 and 20 week ages are always statistically similar ($p>0.05$) for 8N. The 10N tests seem to follow the trends set by 6N. The 8 week age is usually different from the rest of the ages and there are other differences scattered throughout Table 8.

The correlations calculated were all statistically significant ($p < 0.05$). Between the different forces, all parameters show similar Pearson's r values with the exception of US1, AvUS and AvLS. The largest correlations exist for US1, AvUS and AvLS for both 6N and 8N forces, but not for 10N force. Overall, the correlations are weak for RPI tests on different ages of bones.

4.4.2 Osteoprobe measurements

Figure 19 shows BMS measurements plotted against age. Table 10 shows the results of the Tukey test analysis for age differences for BMS. According to the Tukey tests, every age is statistically different from every other age, with the exception of 16 versus 20 weeks. Correlation analysis shows a high values of $r = 0.835$ for BMS versus age.

4.4.3 Three-point bend tests

The three-point bend test properties are plotted against age in Fig. 20. It is worth noting that the statistical differences ($p<0.05$) are only existent between 20 weeks and 4, 8 and 12 weeks for flexural modulus and between 20 weeks and 4, 8, 12 and 16 weeks for strain at break. Table 11 gives the Pearson's r values for correlation between the properties and age. Similar to the statistical differences, the only significant correlations ($p<0.05$) between age and the bend test properties are for flexural modulus and strain at break.

4.4.4 CT scans

Figure 21 shows the change in mineral density, calculated via two methods mentioned above, as a function of age. Tukey test analysis shows no significant differences ($p<0.05$) between the mineral densities for the various ages. Correlation analysis between mineral density and all other measured properties (including age) also showed no significant values ($p<0.05$). Essentially, this analysis shows that mineral density is not changing with age.

4.4.5 Dynamic and static nanoindentation

Figure 22 shows the dynamic portion of the nanoindentation measurements. Only 20 week bone shows a change in properties as the frequency changes. As the frequency is increased to 200Hz, we see that the tan (δ) increases significantly. Figure 23 shows the reduced modulus and hardness as a function of age. All ages show values that are centered on 10GPa, except with 0 weeks we see a sharp increase from the edge until about 80μm, where it peaks at around 23GPa. After that peak, the values drop to around 10GPa, similar to the other ages.

4.4.6 Test correlations

Since the nanoindentation data is being used for qualitative purposes and the CT scan mineral data did not show any correlations, only connections between RPI, BMS and three-point bend test will be analyzed. Table 12 shows the correlation values between RPI and BMS for the various forces used in RPI. With the exception of ID1 and TID for 8N, every correlation is statistically significant. Even though almost every RPI parameter has a significant correlation, the r values are never greater than 0.7, so the correlations are moderately strong at best. The only significant correlation ($p<0.05$) between BMS and the bending properties is with flexural strength. The Pearson's r value for BMS versus flexural strength is -0.510. Out of all the RPI outputs for all three forces, only US1 for 10N shows a significant correlation ($p<0.05$) with flexural strength. All other outputs show low to no correlation and are not significant.

4.5 Discussion

4.5.1 Age differences

From analysis of the data obtained in the study, no clear conclusions can be drawn about the behavior of young porcine cortical bone from tibiae. We would expect, as the bone matures, it

becomes more mineralized and organized, becoming stiffer and stronger in the process to support the added weight of a growing body. Our analysis has shown has shown numerous examples to counteract this thought. If we simply look at Figs. 16-18, we see that the trends change as we change the force and as we change what genetic line we investigate. While we expect some differences between animal lines, the "roller-coaster" ups and downs of some curves (TID for 1050 for example) are highly unexpected. To support the variations seen between forces, the Tukey tests for RPI versus age in Tables 6-8 change with a change in force magnitude. We expect that changing the force would simply adjust the values, but not alter the trends and this is not the case. For 6N and 10N we see that 8 week samples show large deviation from any trends. 8N however, shows that 16 and 20 week samples show the deviation from the group. Also, if we look at correlations, we see that 10N shows lower correlations than the lower forces for some parameters. This does follow what has been shown through a force variation test on 24 week porcine femurs [10]. 10N force magnitude gave significantly different values from other forces [10]. The CT scan mineral density data reinforce this data. Figure 21 shows no significant changes in the mineral density as the bone ages from birth.

Rasoulian et al. tested three ages at or below 24 weeks [9]. Their data shows that 1 month bone was significantly different ($p<0.05$) from all other ages for the same surface tested. In this study, measurements were made in the transverse direction (outer surface) as defined by Rasoulian et al. [9]. The only parameters that can be compared between these studies are IDI, TID, AvED, CID1, Av CID and AvUS since Rasoulian et al. used an older version of the RPI software. There are clear trends visible for IDI, CID1 and AvUS in [9]. The other parameters did not show trends for this age range. 3.5 month (~14 week) and 24 week samples gave values that interrupted any trends. In our study, we also observed a few ages (4, 8 or 12 weeks) that did not follow trends.

This observation could show that RPI may not be a suitable technique to measure differences between ages. The heterogeneity between and within samples for each age may be too large for any trends to develop without hundreds of tests performed per sample. Trends for a wider range of ages, such as that tested by Rasoulian et al., may give better trends since the differences between ages would be more pronounced. RPI has been used to show differences between diseased and healthy tissue [3, 4, 6, 7, 8, 11, 12]. The differences between these two states might also be large enough to overcome sample heterogeneity. The age interval we tested (4 weeks) might also be too small for significant differences to present themselves. At these young ages, bone is being deposited on the outer surface constantly as the bones grow to support the increasing weight of the animal. Any of the bones we have could have been in a stage of bone growth such that the outer surface might not be completely formed, resulting in unexpected results. More insight on this hypothesis can be provided by mineral content measurements and structural images obtained via scanning electron microscopy (SEM) [24].

Is come cases, we see that 0 week bone is just as resistant to indentation as 20 week bone, while the ages in between show less resistance as compared to 20 week bones, as expected. To investigate this, nanoindentation was performed. The dynamic measurements did not show any enlightening data, as only 20 week showed any variation as a function of frequency. The static data, however, did give interesting results. We see that for the 0 week sample, there is a large increase in modulus until about 80μm in from the edge of the sample. All measurements after this depth fall within the range of the other samples. This stiffer outer portion, if present in all bones for 0 week, could account for this 0 week to 20 week RPI similarity. However, since all measurements, aside from this increase, are the same, we would expect 0 week to be stronger than all other ages including 20 weeks. This is not the case. The fact that the nanoindentation

measurements were made on the transverse surface and RPI measurements are made on the longitudinal surface could account for this, as bone is an anisotropic material. In order to determine whether these differences should be considered fact, other measurements and imaging should be done. All other ages and more than one sample per age should be tested with nanoindentation. Again, SEM could give more local mineral density measurements using EDS [24] as well as structural information. Rasoulian et al. did show differences between 4, 14 and 24 week bone using quasi-static nanoindentation [9]. The frequency testing for dynamic measurement that occurred before unloading, used to calculate modulus in our study, may have affected the results. Quasi-static indentation should be done on all samples to show whether or not his is the case.

Three-point bend tests so show some trends for flexural modulus and strain at break, however 0 week is still a sample that ignores the trend. Decreasing the flexural modulus and increasing the strain at break of 0 week samples would provide better trends for those two bending properties. Aside from 0 week samples visually ignoring the trends, 20 week samples were the only ones that showed any significant differences between other samples. Again, this is only for flexural modulus and strain at break. This could show that young bones do not change much in terms of mechanical properties as they develop until they hit a critical age, in this case it would be considered 20 weeks. One could clearly use the 0 week sample's stiff outer portion as a reason for its differences, but the outer surface is cut away when creating bending samples. Again, SEM could help to shed some light on what differences in content and structure could be causing this.

The final property to be explored is BMS measured by the Osteoprobe. The relation between BMS and age showed a rather high Pearson's r value ($|r| > 0.8$) and the Tukey test showed that every age was significantly different ($p<0.05$) from every other one, with the exception of 16 versus 20 weeks. This shows that BMS does show a correlation with age and it is capable of

detecting differences between different age groups. If one looks at Fig. 19, however, it can be seen that either 4 or 8 week samples seem to throw the trend off from being perfect. Tukey tests suggest that it is the 4 week samples since 4 week samples show the highest values for the significant differences present. These small differences could be artifacts and more tests could eliminate these. Overall, BMS seems to be a measure that can detect differences for the whole range of ages.

4.5.2 Test correlations

Since only one correlation existed between RPI and three-point bending as well as for BMS and three-point bending, we can say that three-point bending does not relate to these tests. However, the sample size varied from age to age and that can skew the results. It can also require that additional measures be taken when performing statistical analysis. Further bending tests are needed before a solid conclusion can be drawn.

There are correlations between RPI and BMS however. We expect this since both are similar tests that perform impact indentations. Almost every RPI output showed a significant Pearson's r value when compared to BMS. The correlations are low and this could be due to differences between the two tests. RPI conducts several impact indentations on the same location such that all but the first cycle indent on a damaged surface. Osteoprobe measurements are always done on an undamaged surface and only one cycle is performed. Also, since the number of indents done per bone was limited to 5, heterogeneity in the bones could provide differences between tests. The locations tested with RPI might have different microstructure than those tested with BMS and one test could be more sensitive to variation.

4.6 Summary

In this study, five techniques were used to determine if there were noticeable differences associated with change in age for developing porcine tibiae. Six age groups; 0, 4, 8, 12, 16 and 20 weeks; were analyzed using RPI, the Osteoprobe, three-point bend tests, CT scans and nanoindentation. Mineral content measured by CT scans showed no difference as a function of age. RPI tests showed high variability in the tests, depending on the genetic line that was tested. This, for some RPI parameters, agreed with data from Rasoulian et al. RPI may not be suitable for testing this specific age range. Nanoindentation showed that 0 week bones might have a stiffer outer portion that could give it strength comparable to 20 week samples and only 20 week samples showed any change as a function of frequency. The samples were limited for nanoindentation so more tests would be needed to confirm any observed differences. Quasi-static indentation should be done as well to determine if the dynamic testing affected the modulus measurements. Three-point bend tests only showed correlation to age for flexural modulus and strain at break, and only 20 week samples showed any significant difference to any other age. The varying number of samples per age could account for the low correlations, or lack thereof. Although RPI did not show any clear age related changes, BMS showed promising results. It produced significantly different results for each age, except for 16 versus 20 weeks. It gave a high Pearson's r value of 0.835 indicating moderately strong correlation with age. It did not give strong correlations with RPI, but since RPI itself did not produce expected results, a correlation was not anticipated. There are limitations to this study. More tests are needed to confirm or deny certain results in this work. Imaging techniques like SEM or possibly Raman imaging, could produce enlightening data. Additional samples could also provide more sound analysis, especially for three-point bending and nanoindentation. Other bones, such as femurs, could be used to evaluate the trends presented in

this work. Overall, this work provides a foundation for further research on developing bones and helps validate the clinically approved Osteoprobe device.

CHAPTER 5: GENERAL SUMMARY

Several conclusions were determined throughout this thesis. When using RPI for a 6 month porcine femoral bone it is recommended that testing is done on an unpolished longitudinal surface using 6N force and 20 cycles. Preconditioning has minimal effects on the RPI results and does not affect the trends. We found relatively small variation in the RPI outputs within and between samples. The effect of radiation is not significant on the longitudinal surface and does not affect any important parameters on the transverse surface.

When testing polymers, several correlations were found. The strongest correlations were between RPI and Osteoprobe tests, due to the similarity of the tests. ID1 and TID both show strong inverse correlations to BMS. Other RPI outputs show a moderate to moderately strong correlation to BMS. When it comes to traditional material properties, impact energy shows the strongest correlations, which were anticipated since RPI and Osteoprobe tests are micro-scale impact tests. ID1, TID and the loading and unloading slope outputs, as well as BMS, show the best correlation to Izod impact energy. Elastic and flexural moduli show moderate correlations to the same RPI parameters and BMS. AvCID is the only RPI output to show correlation with elongation at break. Other material properties, such as tensile and flexural strength, show little to no correlation to RPI or Osteoprobe tests. These correlations could improve if we perform our own mechanical tests on the polymers, rather than relying on material data sheets.

The age study showed some interesting results, but changes were detected for only a few of the tests. Mineral content measured by CT scans showed no difference as a function of age. RPI tests showed high variability in the tests, depending on the genetic line that was tested. This was in general agreement with previous work [9]. RPI may not be suitable to determine differences in this particular age range. Nanoindentation showed that 0 week bones might have a stiffer outer

portion that could give it strength comparable to 20 week samples and 20 week samples showed an increase in tan (δ) as the frequency neared 200Hz. The samples were limited for nanoindentation so more tests would be needed to confirm any observed differences. Quasi-static indentation should also be done to determine if dynamic measurements have any effect on static measurement parameters like reduced modulus. Three-point bend tests showed correlation to age for flexural modulus and strain at break, however only 20 week samples showed any significant difference to any other age. The varying number of samples per age could explain the lack of significant differences. BMS showed the most promising results. It produced significantly different results for each age, except for 16 versus 20 weeks. It gave a high Pearson's r value of 0.835 indicating moderately strong correlation with age. It did not give strong correlations with RPI, but since RPI itself did not produce expected results, a correlation was not anticipated.

More work can be done to solidify conclusions mentioned above. Increasing the number of samples tested, in the case of bending and nanoindentation tests for example, could give more reliable and significant data for analysis. Analyzing other bones, such as femurs or upper limb bones, could provide insight into RPI's significance in determining age related changes as well as its relation to other, more destructive test methods. Testing these other bones could also solidify the BMS parameter as a viable predictor of bone properties. Finally, testing additional standard materials that cover a range of material property values, as well as testing for other material properties like fracture toughness, would help develop the fundamental understanding of both RPI and BMS measurements.

While there are limitations and areas where future work would be beneficial, this thesis shows that changes are present in porcine cortical bone as it develops. The properties did not consistently improve with age as expected, opening a new area of investigation: the structural and

compositional factors that make 0 week bone comparable to 20 week bone. This thesis also presents the RPI technique as possible tool to analyze these changes without the need for excised tissue. More work is needed to determine the validity of the technique, but the method is promising.

CHAPTER 6: ADDITIONAL COLLABORATIVE WORK

Two collaborative works with colleagues from the University of Denver have been published in which I performed nanoindentation measurements. The purpose of these works was to determine the effects that high temperatures and/or ozone had on polymer epoxies. Nanoindentation was performed to determine the extent of property change as a function of depth from the material surface. These works are listed as references [25] and [26].

CHAPTER 7: REFERENCES

[1] A. I. Pearce, R. G. Richards, E. Schneider and S. G. Pearce, "Animal models for implant biomaterial research in bone: a review," *European Cells and Materials,* vol. 13, pp. 1-10, 2007.

[2] P. K. Hansma, P. J. Turner and G. E. Fantner, "Bone diagnostic instrument," *Review of Scientific Instruments,* vol. 77, pp. 1-6, 2006.

[3] P. Hansma, P. Turner, B. Drake, E. Yurtsev, A. Proctor, P. Mathews, J. Lulejian, C. Randall, J. Adams, R. Jungmann, F. Garza-de-Leon, G. Fantner, H. Mkrtchyan, M. Pontin, A. Weaver, M. B. Brown, N. Sahar, R. Rossello and D. Kohn, "The bone diagnostic instrument II: indentation distance increase," *Review of Scientific Instruments,* vol. 79, pp. 1-8, 2008.

[4] C. Randall, P. Mathews, E. Yurtsev, N. Sahar, D. Kohn and P. Hansma, "The bone diagnostic instrument III: Testing mouse femora," *Review of Scientific Instruments,* vol. 80, pp. 1-3, 2009.

[5] D. Bridges, C. Randall and P. K. Hansma, "A new device for performing reference point indentation without a reference probe," *Review of Scientific Instruments,* vol. 83, pp. 1-8, 2012.

[6] A. Diez-Perez, R. Guerri, X. Nogues, E. Caceres, M. J. Pena, L. Mellibovsky, C. Randall, D. Bridges, J. C. Weaver, A. Proctor, D. Brimer, K. J. Koester, R. O. Ritchie and P. K. Hansma, "Microindentation for In Vivo Measurement of Bone Tissue Mechanical Properties in Humans," *Journal of Bone and Mineral Research,* vol. 25, no. 8, pp. 1877-1885, August 2010.

[7] R. C. Guerri-Fernandez, X. Nogues, J. M. Quesada Gomez, E. Torres del Pliego, L. Puig, N. Garcia-Giralt, G. Yoskovitz, L. Mellibovsky, P. K. Hansma and A. Diez-Perez, "Micronidentation for In Vivo Measurement of Bone Tissue Material Properties in Atypical Femoral Fracture Patients and Controls," *Journal of Bone and Mineral Research,* vol. 28, no. 1, pp. 162-168, 2013.

[8] M. A. Gallant, D. M. Brown, J. M. Organ, M. R. Allen and D. B. Burr, "Reference-point indentation correlates with bone toughness assessed using whole-bone traditional mechanical testing," *Bone,* vol. 53, pp. 301-305, 2013.

[9] R. Rasoulian, A. Raeisi Najafi, M. Chittenden and I. Jasiuk, "Reference point indentation study of age-related changes in porcine femoral cortical bone," *Journal of Biomechanics,* vol. 46, pp. 1689-1696, 2013.

[10] A. Setters and I. Jasiuk, "Towards a standardized reference point indentation testing procedure," *Journal of the Mechanical Behavior of Biomedical Materials,* vol. 34, pp. 57-65, 2014.

[11] M. Aref, M. A. Gallant, J. M. Organ, J. M. Wallace, C. L. Newman, D. B. Burr, D. M. Brown and M. R. Allen, "In vivo reference point indentation reveals positive effects of raloxifene on mechanical properties following 6 months of treatment in skeletally mature beagle dogs," *Bone,* vol. 56, pp. 449-453, 2013.

[12] M. Granke, A. Coulmier, S. Uppuganti, J. A. Gaddy, M. D. Does and J. S. Nyman, "Insights into reference point indentation involving human cortical bone: Sensitivity to tissue anisotropy and mechancial behavior," *Journal of the Mechanical Behavior of Biomedical Materials,* vol. 37, pp. 174-185, 2014.

[13] S. Y. Tang, P. Mathews, C. Randall, E. Yurtsev, K. Fields, A. Wong, A. C. Kuo, T. Alliston and P. Hansma, "In situ materials characterization using the tissue diagnostic instrument," *Polymer Testing,* vol. 29, pp. 159-163, 2010.

[14] C. Randall, D. Bridges, R. Guerri, X. Nogues, L. Puig, E. Torres, L. Mellibovsky, K. Hoffseth, T. Stalbaum, A. Srikanth, J. C. Weaver, S. Rosen, H. Bamard, D. Brimer, A. Proctor, J. Candy, C. Saldana, S. Chandrasekar, T. Lescun, C. M. Neilson, E. Orwoll, D. Herthel, H. Kopeikin, H. T. Yang, J. N. Farr, L. McCready, S. Khosla, A. Diez-Perez and P. K. Hansma, "Applications of a New Handheld Reference Point Indentation Instrument Measuring Bone Material Strength," *Journal of Medical Devices,* vol. 7, pp. 1-6, 2013.

[15] E. Torres del Pliego, L. Vilaplana, R. Guerri-Fernandez and A. Diez-Perez, "Measuring Bone Quality," *Curr Rheumatol Rep,* vol. 15, no. 373, pp. 1-7, 2013.

[16] J. N. Farr, M. T. Drake, S. Amin, J. Melton III, L. K. McCready and S. Khosla, "In Vivo Assessment of Bone Quality in Postmenopausal Women With Type 2 Diabetes," *Journal of Bone and Mineral Research,* vol. 29, no. 4, pp. 787-795, 2014.

[17] "Acrylic," eFunda, 2014. [Online]. Available: http://www.efunda.com/materials/polymers/properties/polymer_datasheet.cfm?MajorID=acrylic&MinorID=4. [Accessed 9 July 2014].

[18] J. P. Berteau, C. Baron, M. Pithioux, F. Launay, P. Chabrand and P. Lasaygues, "In vitro ultrasonic and mechanic characterization of the modulus of elasticity of children cortical bone," *Ultrasonics,* vol. 54, pp. 1270-1276, 2013.

[19] C. I. Albert, J. Jameson and G. Harris, "Design and validation of bending test method for characterization of miniature pediatric cortical bone specimens," *Journal of Engineering in Medicine,* vol. 227, no. 2, pp. 105-113, 2012.

[20] C. Wang, H. Frimmel and O. Smedby, "Level-set based vessel segmentation accelerated with periodic monotonic speed function," *Medical Imaging,* vol. 7962, no. 1M, pp. 1-7, 2011.

[21] E. Schileo, E. Dall'Ara, F. Taddei, A. Malandrino, T. Schotkamp, M. Baleani and M. Viceconti, "An accurate estimation of bone density improves the accuracy of subject-specific finite element models," *Journal of Biomechanics* , vol. 41, pp. 2483-2491, 2008.

[22] M. Crookshank, H. L. Ploeg, R. Ellis and N. J. MacIntyre, "Repeatable calibration of Hounsfield units to mineral density and effect of scanning medium," *Advances in Biomechanics and Applications,* vol. 1, no. 1, pp. 015-022, 2014.

[23] S. P. Singh, J. F. Smith and R. P. Singh, "Characterization of the Damping Behavior of a Nanoindentation Instrument for Carrying Out Dynamic Experiments," *Experimental Mechanics,* vol. 48, pp. 571-583, 2008.

[24] C. K. Tjhia, C. V. Odvina, D. S. Rao, S. M. Stover, X. Wang and D. P. Fyhrie, "Mechanical property and tissue density differences among severely suppressed bone turnover (SSBT) patients, osteoporotic patients, and normal subjects," *Bone,* vol. 49, pp. 1279-1289, 2011.

[25] J. Middleton, B. Burks, T. Wells, A. M. Setters, I. Jasiuk, P. Predecki, J. Hoffman and M. Kumosa, "The effect of ozone on polymer degradation in Polymer Core Composite Conductors," *Polymer Degradation and Stability,* vol. 98, pp. 436-445, 2013.

[26] J. Middleton, B. Burks, T. Wells, A. M. Setters, I. Jasiuk and M. Kumosa, "The effect of ozone and high temperature on polymer degradation in polymer core composite conductors," *Polymer Degradation and Stability,* vol. 98, pp. 2282-2290, 2013.

CHAPTER 8: TABLES

Table 1: Description of the RPI outputs.

RPI Output	Description
ID1	Test probe penetration depth for the first test cycle
US1	Unloading slope for the first test cycle
CID1	Creep indentation distance for the first test cycle
TID	Total test probe penetration depth
IDI	Increase in penetration depth from the first test cycle to the last test cycle
AvCID	Average of the creep indentation distance over all test cycles
AvED	Average of the energy dissipated (area under the test curve) over the 3rd to the last test cycle
AvUS	Average of the unloading slope over all test cycles
AvLS	Average of the loading slope over all test cycles

Table 2: Tukey test results for the IDI parameter for the force variation test (p=0.05).

IDI				
	2N	4N	6N	8N
4N	0.373			
6N	0.288	> 0.999		
8N	0.157	0.987	0.997	
10N	**< 0.001**	**0.002**	**0.004**	**0.009**

Table 3: Tukey test results for the cycle variation test (p=0.05).

ID1					TID					AvED				
	2	5	10	15		2	5	10	15		2	5	10	15
5	0.995				5	0.872				5	NaN			
10	0.219	0.101			10	**< 0.001**	**0.006**			10	NaN	0.085		
15	0.712	0.469	0.904		15	**0.005**	0.060	0.913		15	NaN	**0.015**	0.886	
20	**0.015**	**0.005**	0.768	0.260	20	**< 0.001**	**< 0.001**	0.151	**0.021**	20	NaN	**0.007**	0.750	0.993
US1					IDI					AvUS				
	2	5	10	15		2	5	10	15		2	5	10	15
5	0.963				5	**< 0.001**				5	> 0.999			
10	**0.012**	0.065			10	**< 0.001**	**< 0.001**			10	0.139	0.139		
15	0.090	0.322	0.925		15	**< 0.001**	**0.013**	0.730		15	0.881	0.881	0.602	
20	0.999	0.992	**0.022**	0.144	20	**< 0.001**	**< 0.001**	0.645	0.085	20	0.864	0.864	**0.013**	0.325
CID1					AvCID					AvLS				
	2	5	10	15		2	5	10	15		2	5	10	15
5	0.990				5	**< 0.001**				5	**< 0.001**			
10	0.625	0.880			10	**< 0.001**	**<0.001**			10	**< 0.001**	0.792		
15	0.343	0.149	**0.016**		15	**< 0.001**	**< 0.001**	**< 0.001**		15	**< 0.001**	**0.013**	0.180	
20	0.343	0.149	**0.016**	> 0.999	20	**< 0.001**	**< 0.001**	**< 0.001**	0.181	20	**< 0.001**	**< 0.001**	**< 0.001**	0.154
BOLD indicates the difference is statistically significant at the 0.05 level														
For AvED, at least 3 cycles is needed (The program averages over the 3rd through last cycles). Thus, 2 cycles doesn't have a value.														

Table 4: Mechanical properties of select polymers

Polymer	Tens Str (MPa)	Elast Mod (GPa)	Elong Brk (%)	Flex Str (MPa)	Flex Mod (GPa)	Izod Notch Imp (J/m)	Density (g/cm^3)
ABS	36.00	2.40	4.00	61.00	2.30	139.00	1.037
FC720	57.50	2.50	20.00	95.00	3.00	25.00	1.185
PA	46.00	1.65	13.30	N/A	1.50	N/A	0.930
PC	68.00	2.30	5.00	104.00	2.20	53.00	1.197
PC-ABS	41.00	1.90	6.00	68.00	1.90	196.00	1.097
PMMA	60.00	2.85	4.00	101.50	2.70	1.50	1.182
PG	43.00	2.25	12.00	68.60	2.06	21.00	1.160
VW	57.50	2.50	20.00	92.50	2.70	25.00	1.175
WCU	55.50	2.88	7.50	83.50	2.49	25.00	1.130

Table 5: Pearson's r values for polymer correlation tests. **Bold** values indicate statistical significance ($p < 0.05$).

	Tens. Str. (MPa)	Elast. Mod. (GPa)	Elong. at Brk. (%)	Flex. Str. (MPa)	Flex. Mod. (GPa)	Izod Impact (J/m)
ID1 (µm)	**-0.495**	**-0.689**	-0.154	**-0.485**	-0.059	**0.871**
US1 (N/µm)	**0.313**	**0.703**	0.213	**0.377**	0.231	**-0.739**
CID1 (µm)	**-0.408**	-0.167	0.270	**-0.357**	0.049	**0.497**
TID (µm)	**-0.451**	**-0.654**	-0.102	**-0.427**	-0.017	**0.832**
IDI (µm)	-0.081	0.056	0.290	-0.011	0.176	0.257
AvCID (µm)	**0.383**	-0.018	**0.732**	**0.394**	0.263	-0.128
AvED (µJ)	0.134	**-0.643**	0.239	0.116	0.056	0.244
AvUS (N/µm)	**0.331**	**0.715**	0.279	**0.375**	0.201	**-0.756**
AvLS (N/µm)	0.220	**0.771**	-0.017	0.290	0.068	**-0.501**
BMS (-)	**0.465**	**0.781**	0.030	**0.481**	0.030	**-0.855**

Table 6: Tukey test results of age differences for 6N RPI outputs. **Bold** entries are statistically significant ($p < 0.05$).

ID1						TID						AvED					
	0	4	8	12	16		0	4	8	12	16		0	4	8	12	16
4	0.194	--	--	--	--	4	0.076	--	--	--	--	4	**<0.001**	--	--	--	--
8	**0.028**	**<0.001**	--	--	--	8	**0.049**	**<0.001**	--	--	--	8	1.000	**<0.001**	--	--	--
12	0.383	0.999	**<0.001**	--	--	12	0.310	0.984	**<0.001**	--	--	12	**0.028**	0.863	**0.027**	--	--
16	0.661	0.962	**<0.001**	0.999	--	16	0.424	0.952	**<0.001**	1.000	--	16	**<0.001**	1.000	**<0.001**	0.884	--
20	**0.046**	0.989	**<0.001**	0.915	0.701	20	**0.009**	0.975	**<0.001**	0.714	0.588	20	**<0.001**	0.755	**<0.001**	0.138	0.725
US1						IDI						AvUS					
	0	4	8	12	16		0	4	8	12	16		0	4	8	12	16
4	0.227	--	--	--	--	4	**<0.001**	--	--	--	--	4	0.093	--	--	--	--
8	0.999	0.486	--	--	--	8	0.994	**<0.001**	--	--	--	8	0.951	0.477	--	--	--
12	0.059	0.990	0.175	--	--	12	0.243	0.271	0.074	--	--	12	**0.028**	0.997	0.227	--	--
16	**0.008**	0.772	**0.031**	0.979	--	16	**0.020**	0.874	**0.004**	0.903	--	16	**0.001**	0.731	**0.024**	0.936	--
20	**<0.001**	0.175	**0.001**	0.486	0.896	20	**<0.001**	0.782	**<0.001**	0.011	0.162	20	**<0.001**	0.060	**<0.001**	0.172	0.694
CID1						AvCID						AvLS					
	0	4	8	12	16		0	4	8	12	16		0	4	8	12	16
4	**0.004**	--	--	--	--	4	**0.002**	--	--	--	--	4	**0.020**	--	--	--	--
8	1.000	**0.002**	--	--	--	8	1.000	**0.001**	--	--	--	8	0.998	0.067	--	--	--
12	0.147	0.796	0.097	--	--	12	**0.049**	0.879	**0.039**	--	--	12	**0.037**	1.000	0.113	--	--
16	**0.039**	0.978	**0.023**	0.994	--	16	**0.003**	1.000	**0.002**	0.931	--	16	**<0.001**	0.867	**0.002**	0.755	--
20	**<0.001**	0.882	**<0.001**	0.177	0.455	20	**<0.001**	0.853	**<0.001**	0.220	0.778	20	**<0.001**	**0.035**	**<0.001**	**0.019**	0.398

Table 7: Tukey test results of age differences for 8N RPI outputs. **Bold** entries are statistically significant ($p < 0.05$).

ID1						TID						AvED					
	0	4	8	12	16		0	4	8	12	16		0	4	8	12	16
4	0.904	--	--	--	--	4	0.926	--	--	--	--	4	0.700	--	--	--	--
8	**0.048**	0.409	--	--	--	8	**0.035**	0.308	--	--	--	8	0.901	0.999	--	--	--
12	**0.019**	0.237	0.999	--	--	12	**0.011**	0.142	0.999	--	--	12	0.308	**0.009**	**0.029**	--	--
16	0.877	0.276	**0.002**	**<0.001**	--	16	0.702	0.164	**<0.001**	**<0.001**	--	16	**<0.001**	**0.023**	**0.007**	**<0.001**	--
20	0.462	0.060	**<0.001**	**<0.001**	0.980	20	0.260	**0.027**	**<0.001**	**<0.001**	0.977	20	**<0.001**	**0.002**	**<0.001**	**<0.001**	0.980
US1						IDI						AvUS					
	0	4	8	12	16		0	4	8	12	16		0	4	8	12	16
4	0.737	--	--	--	--	4	0.988	--	--	--	--	4	0.371	--	--	--	--
8	0.717	1	--	--	--	8	0.879	0.514	--	--	--	8	0.412	1	--	--	--
12	0.973	0.276	0.259	--	--	12	0.518	0.183	0.989	--	--	12	1.000	0.523	0.568	--	--
16	**<0.001**	**0.005**	**0.006**	**<0.001**	--	16	0.053	0.220	**0.002**	**<0.001**	--	16	**<0.001**	**0.007**	**0.005**	**<0.001**	--
20	**<0.001**	**<0.001**	**<0.001**	**<0.001**	0.968	20	**0.003**	**0.022**	**<0.001**	**<0.001**	0.930	20	**<0.001**	**<0.001**	**<0.001**	**<0.001**	0.922
CID1						AvCID						AvLS					
	0	4	8	12	16		0	4	8	12	16		0	4	8	12	16
4	0.987	--	--	--	--	4	0.788	--	--	--	--	4	0.449	--	--	--	--
8	0.987	0.794	--	--	--	8	1.000	0.863	--	--	--	8	0.567	1	--	--	--
12	0.395	0.118	0.794	--	--	12	0.086	**0.002**	0.059	--	--	12	1.000	0.316	0.421	--	--
16	0.149	0.461	**0.031**	**<0.001**	--	16	**<0.001**	**0.021**	**<0.001**	**<0.001**	--	16	**<0.001**	**0.013**	**0.007**	**<0.001**	--
20	**0.001**	**0.009**	**<0.001**	**<0.001**	0.529	20	**<0.001**	**0.001**	**<0.001**	**<0.001**	0.960	20	**<0.001**	**0.004**	**0.002**	**<0.001**	0.998

Table 8: Tukey test results of age differences for 10N RPI outputs. **Bold** entries are statistically significant ($p < 0.05$).

ID1						TID						AvED					
	0	4	8	12	16		0	4	8	12	16		0	4	8	12	16
4	**0.009**	--	--	--	--	4	**0.035**	--	--	--	--	4	1.000	--	--	--	--
8	**<0.001**	**0.014**	--	--	--	8	**<0.001**	**0.003**	--	--	--	8	0.132	0.218	--	--	--
12	0.325	0.692	**<0.001**	--	--	12	0.498	0.786	**<0.001**	--	--	12	0.219	0.132	**<0.001**	--	--
16	0.993	**0.001**	**<0.001**	0.105	--	16	0.971	**0.003**	**<0.001**	0.126	--	16	0.237	0.145	**<0.001**	1.000	--
20	0.896	**<0.001**	**<0.001**	**0.030**	0.996	20	0.791	**<0.001**	**<0.001**	**0.035**	0.996	20	**0.033**	**0.017**	**<0.001**	0.966	0.959
US1						IDI						AvUS					
	0	4	8	12	16		0	4	8	12	16		0	4	8	12	16
4	0.268	--	--	--	--	4	1.000	--	--	--	--	4	**0.002**	--	--	--	--
8	0.975	0.051	--	--	--	8	**<0.001**	**<0.001**	--	--	--	8	0.989	**<0.001**	--	--	--
12	**0.007**	0.694	**<0.001**	--	--	12	0.984	0.995	**<0.001**	--	--	12	**<0.001**	0.999	**<0.001**	--	--
16	0.386	1.000	0.088	0.552	--	16	0.255	0.331	**<0.001**	0.659	--	16	0.139	0.705	**0.030**	0.490	--
20	**0.036**	0.950	**0.004**	0.993	0.879	20	0.171	0.230	**<0.001**	0.526	1.000	20	**0.004**	1.000	**<0.001**	0.995	0.813
CID1						AvCID						AvLS					
	0	4	8	12	16		0	4	8	12	16		0	4	8	12	16
4	0.889	--	--	--	--	4	0.988	--	--	--	--	4	0.548	--	--	--	--
8	**<0.001**	**0.004**	--	--	--	8	**0.001**	**0.010**	--	--	--	8	0.931	0.100	--	--	--
12	0.996	0.609	**<0.001**	--	--	12	0.394	0.119	**<0.001**	--	--	12	**0.003**	0.282	**<0.001**	--	--
16	0.082	**0.004**	**<0.001**	0.244	--	16	0.057	**0.010**	**<0.001**	0.936	--	16	0.440	1.000	0.067	0.373	--
20	0.107	**0.005**	**<0.001**	0.299	1.000	20	**0.018**	**0.002**	**<0.001**	0.746	0.998	20	**0.009**	0.440	**<0.001**	1.000	0.548

Table 9: Pearson's r values for RPI-age correlations for each force. All values are statistically significant ($p < 0.05$).

	Age (6N)	Age (8N)	Age (10N)
ID1	-0.254	-0.227	-0.285
US1	0.463	0.516	0.300
CID1	-0.373	-0.367	-0.396
TID	-0.285	-0.256	-0.293
IDI	-0.392	-0.373	-0.325
AvCID	-0.418	-0.429	-0.440
AvED	-0.445	-0.440	-0.411
AvUS	0.514	0.562	0.287
AvLS	0.534	0.507	0.354

Table 10: Tukey test results of age differences for BMS. **Bold** values indicate statistical significance ($p < 0.05$).

BMS					
	0	4	8	12	16
4	**<0.001**	--	--	--	--
8	**<0.001**	**0.001**	--	--	--
12	**<0.001**	**0.040**	**<0.001**	--	--
16	**<0.001**	**<0.001**	**<0.001**	**<0.001**	--
20	**<0.001**	**<0.001**	**<0.001**	**<0.001**	0.999

Table 11: Pearson's r values for three-point bend test properties versus age. **Bold** values indicate statistical significance ($p < 0.05$).

	Pearson's r
Flexural Modulus	**0.607**
Flexural Strength	0.085
Flexural Toughness	-0.233
Strain @ Break	**-0.497**

Table 12: Pearson's r correlation values between BMS and RPI outputs for each age. **Bold** values indicate statistical significance ($p < 0.05$).

	BMS (6N)	BMS (8N)	BMS (10N)
ID1	**-0.508**	-0.375	**-0.470**
US1	**0.553**	**0.642**	**0.582**
CID1	**-0.580**	**-0.564**	**-0.659**
TID	**-0.536**	-0.404	**-0.494**
IDI	**-0.608**	**-0.559**	**-0.638**
AvCID	**-0.652**	**-0.573**	**-0.700**
AvED	**-0.688**	**-0.564**	**-0.663**
AvUS	**0.626**	**0.675**	**0.571**
AvLS	**0.668**	**0.648**	**0.601**

CHAPTER 9: FIGURES

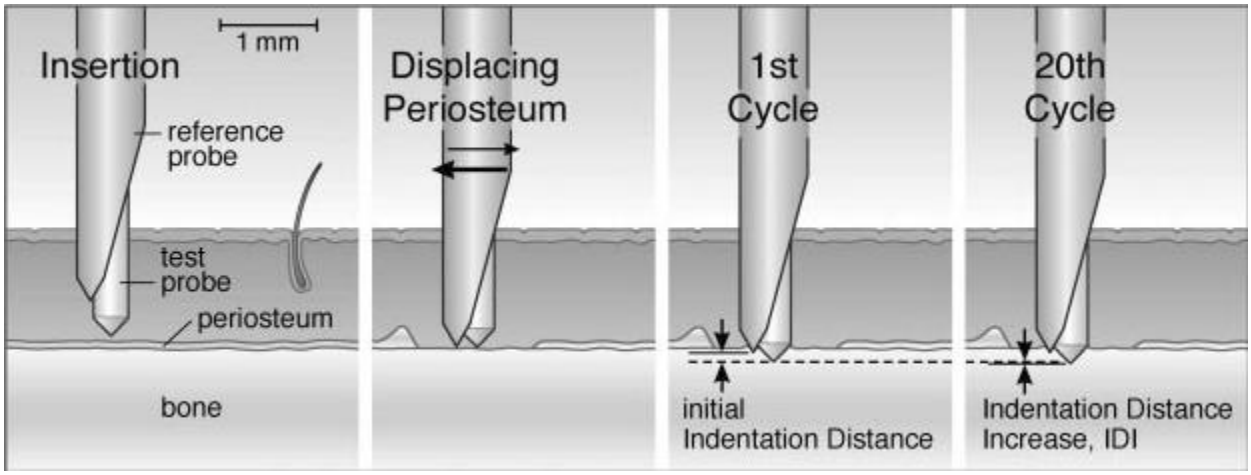

Figure 1: Diagram of an RPI test [4].

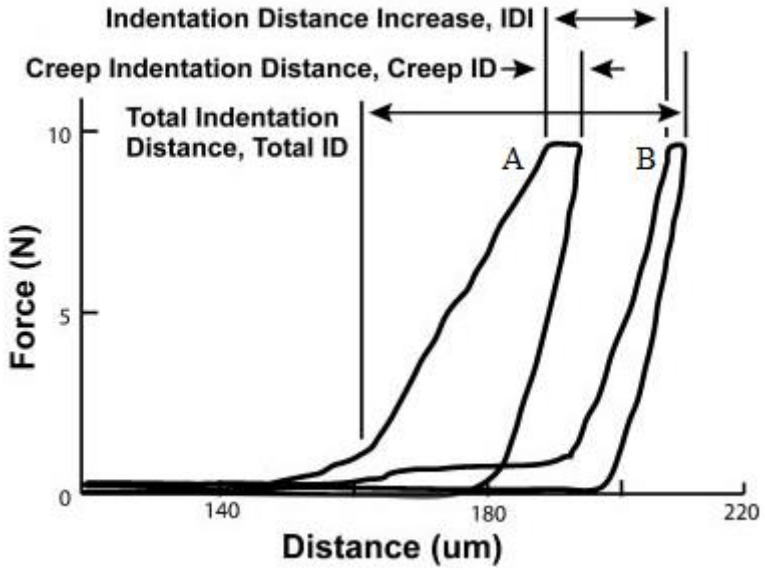

Figure 2: Plot showing A) the first cycle curve and B) the last cycle curve of a typical RPI test [4].

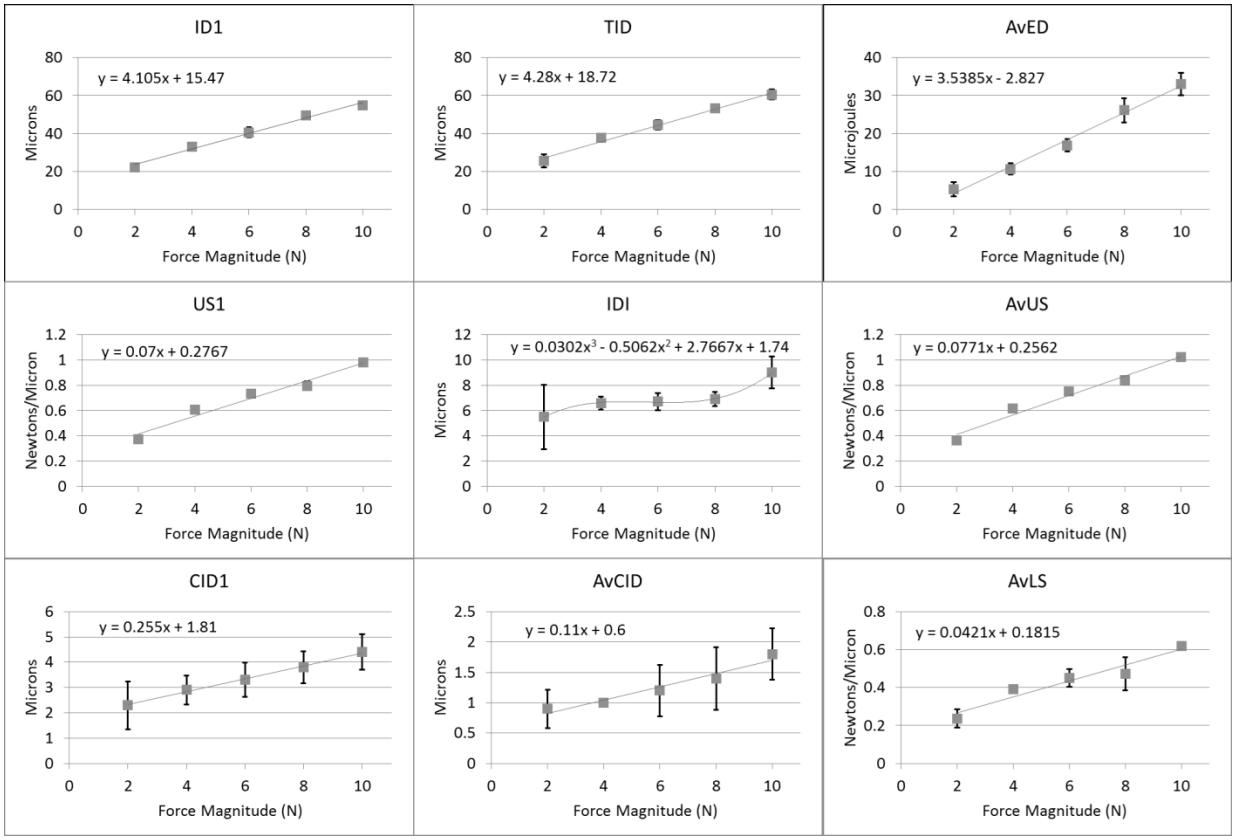

Figure 3: RPI outputs as a function of force magnitude. Bars indicate standard deviation.

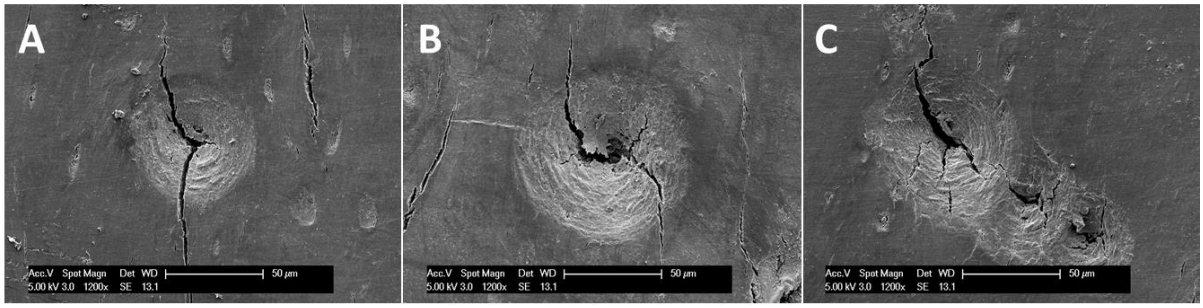

Figure 4: SEM images of: A) a 2N indent, B) a 4N indent and C) an indent showing the "skipping" that can occur for an indentation force of 2N. The scale bar indicates 50 µm.

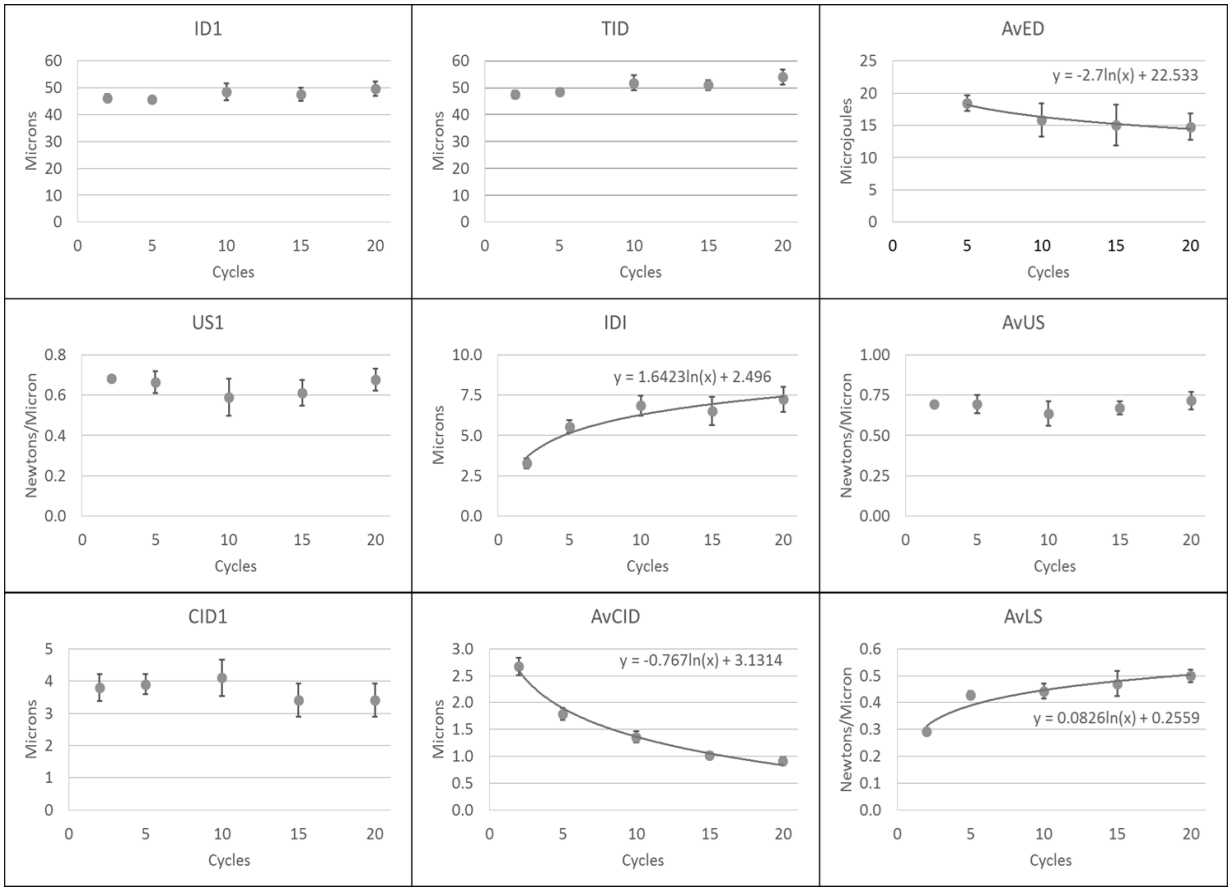

Figure 5: RPI outputs as a function of number of cycles. Bars indicate standard deviation. Note that some results show very small standard deviation.

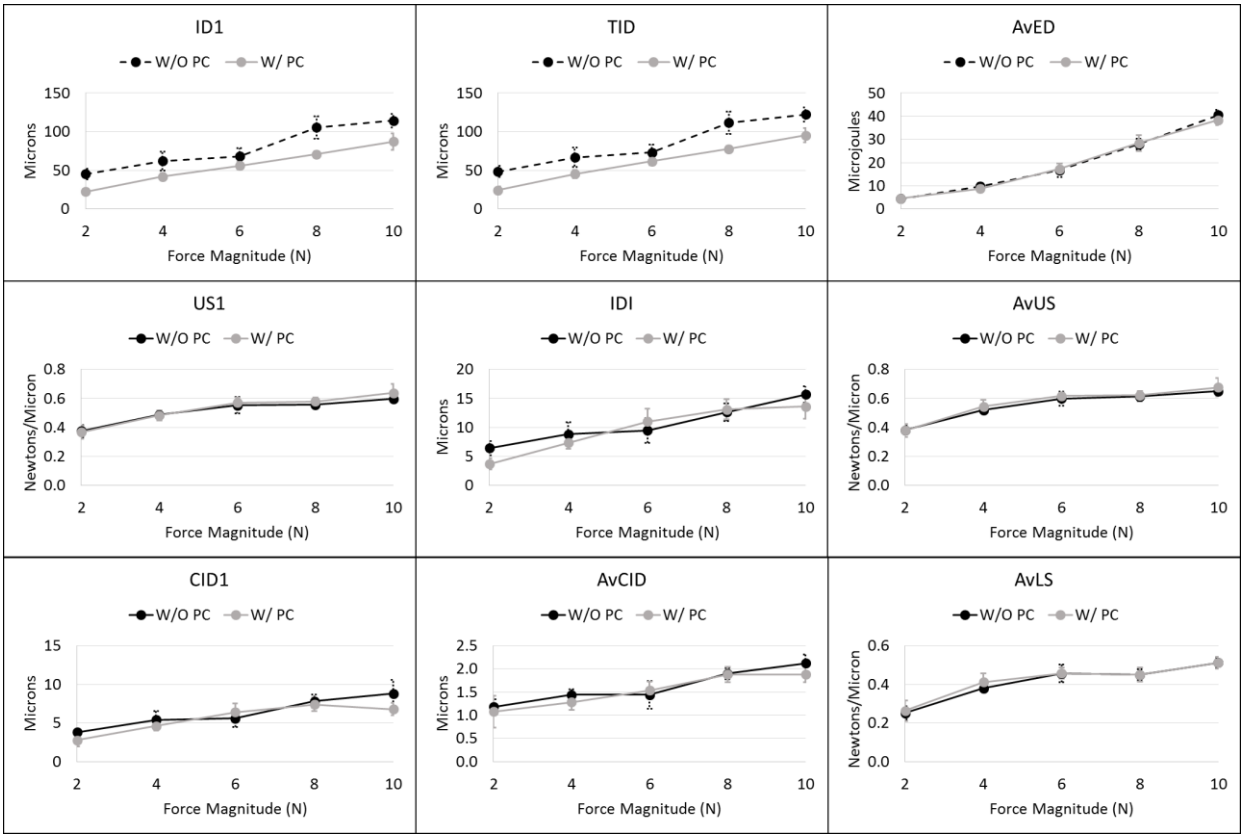

Figure 6: RPI outputs as a function of preconditioning and force magnitude. W/O PC is the test without preconditioning and W/ PC is the test with preconditioning. Bars indicate standard deviation.

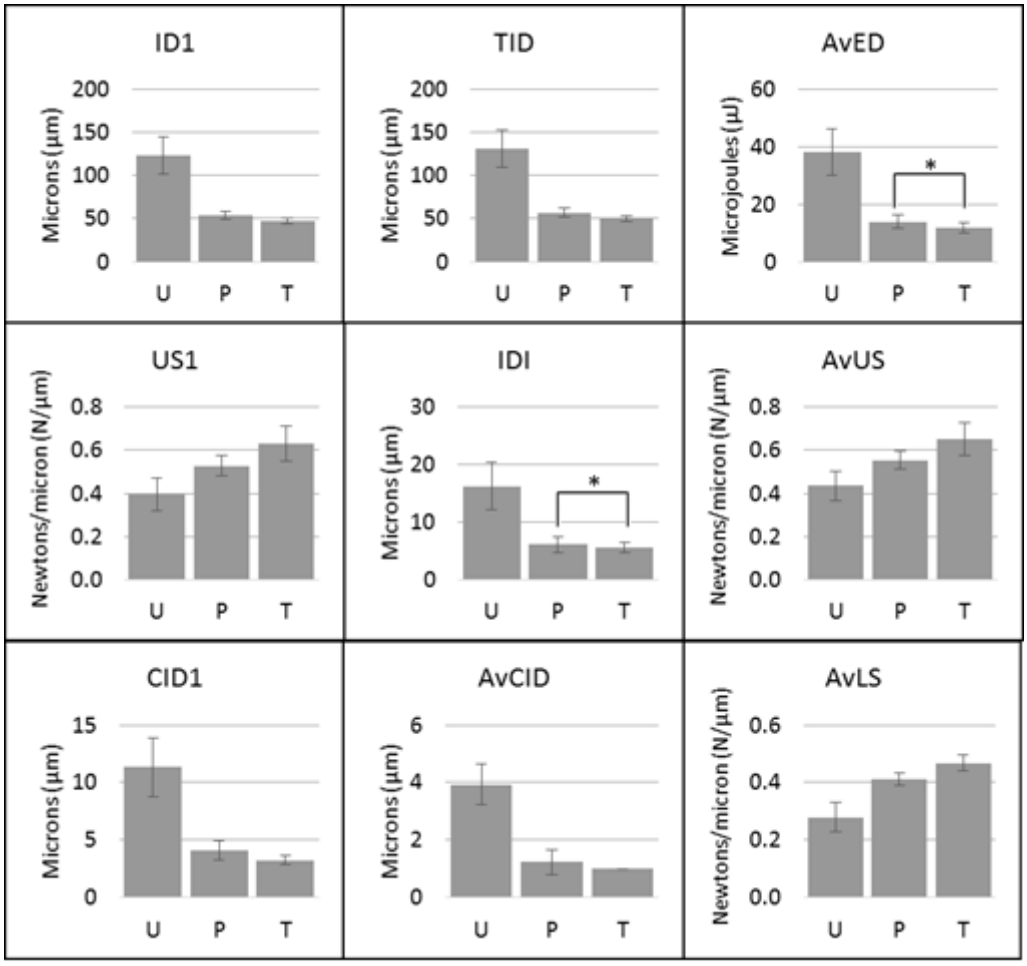

Figure 7: RPI outputs as a function of surface (U = unpolished longitudinal, P = polished longitudinal, T = polished transverse). Bars indicate standard deviation. A '*' indicates no significant difference ($p>0.05$).

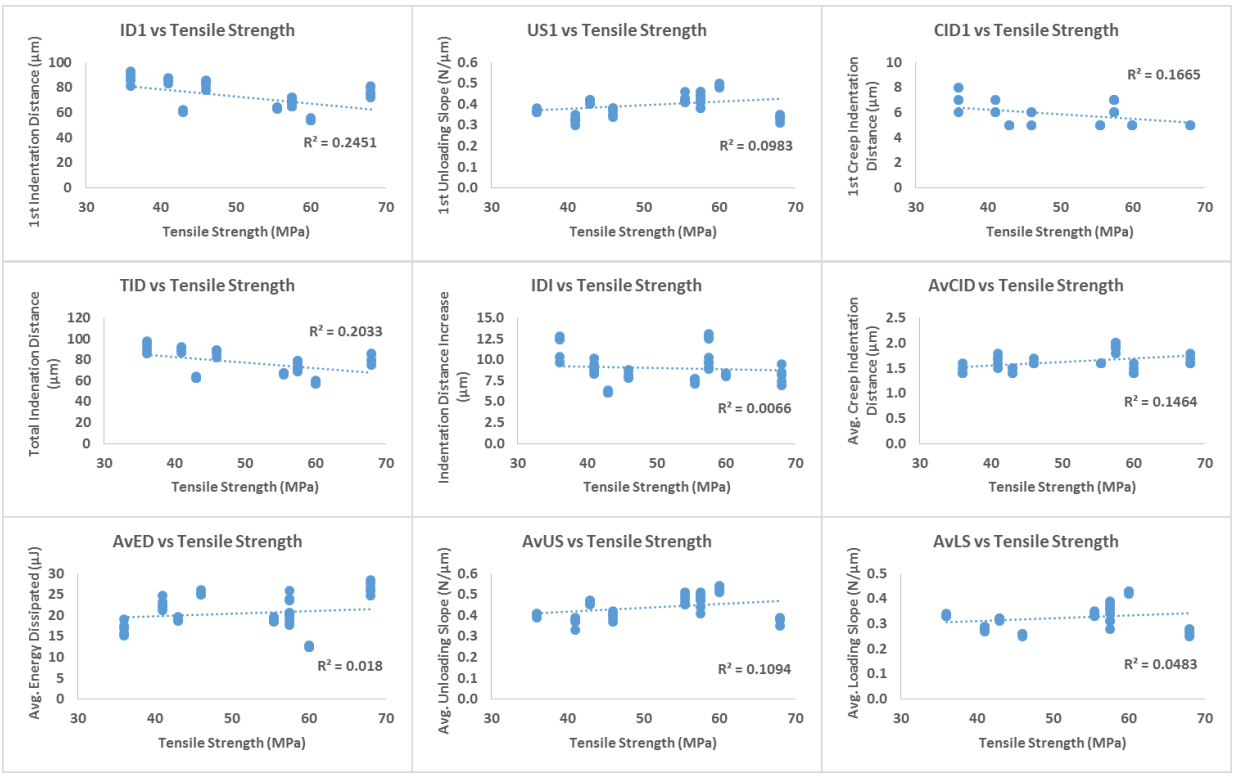

Figure 8: RPI outputs versus tensile strength.

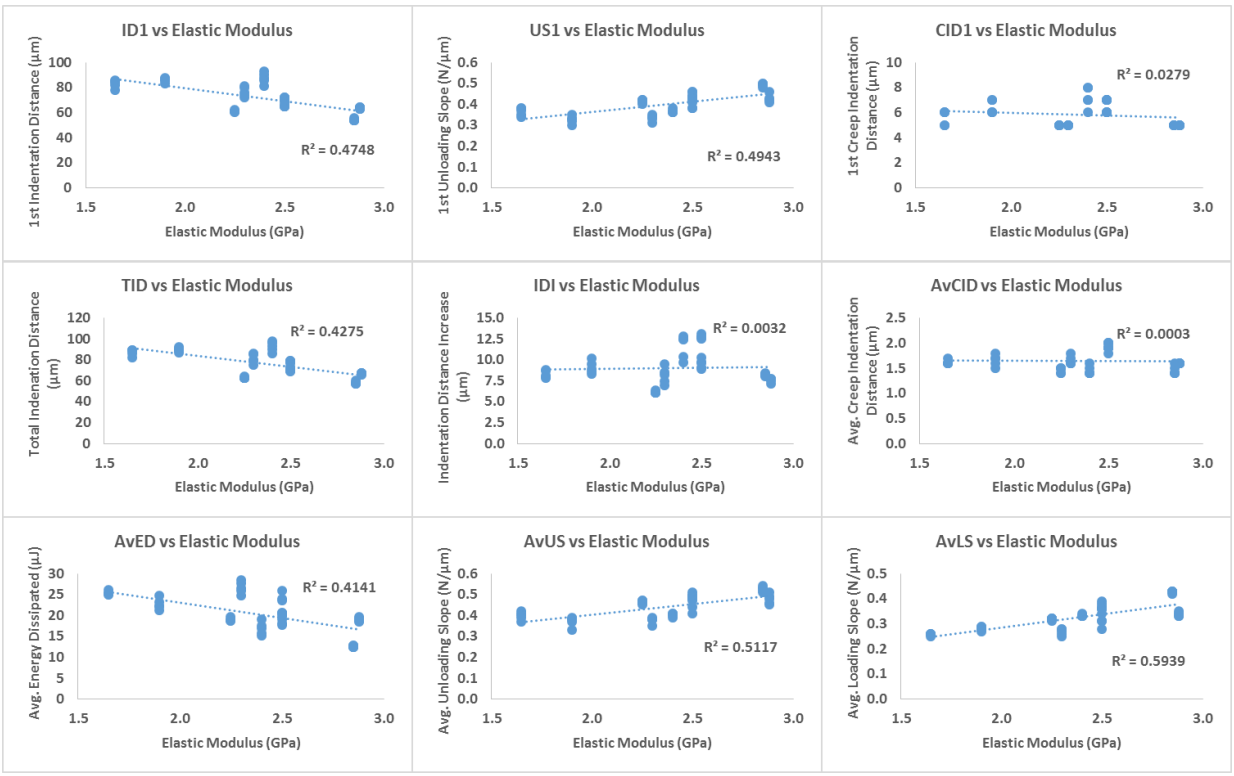

Figure 9: RPI outputs versus elastic modulus.

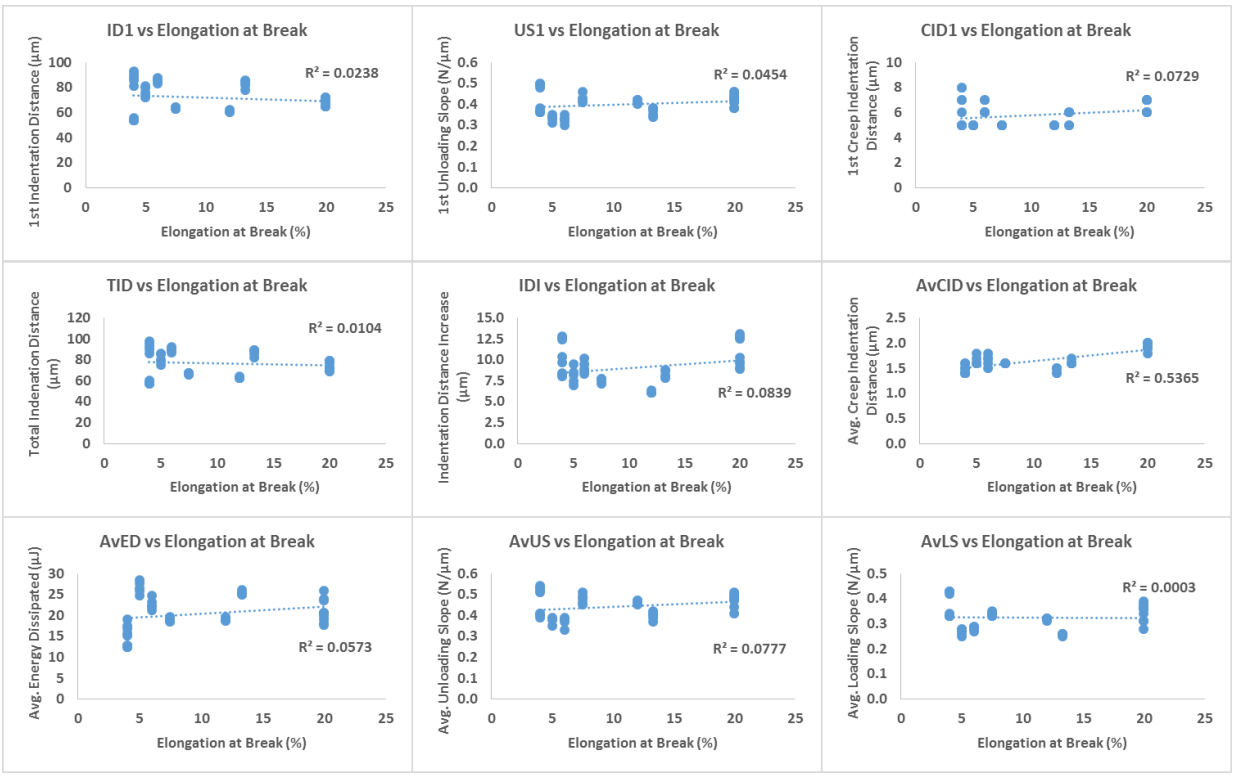

Figure 10: RPI outputs versus elongation at break.

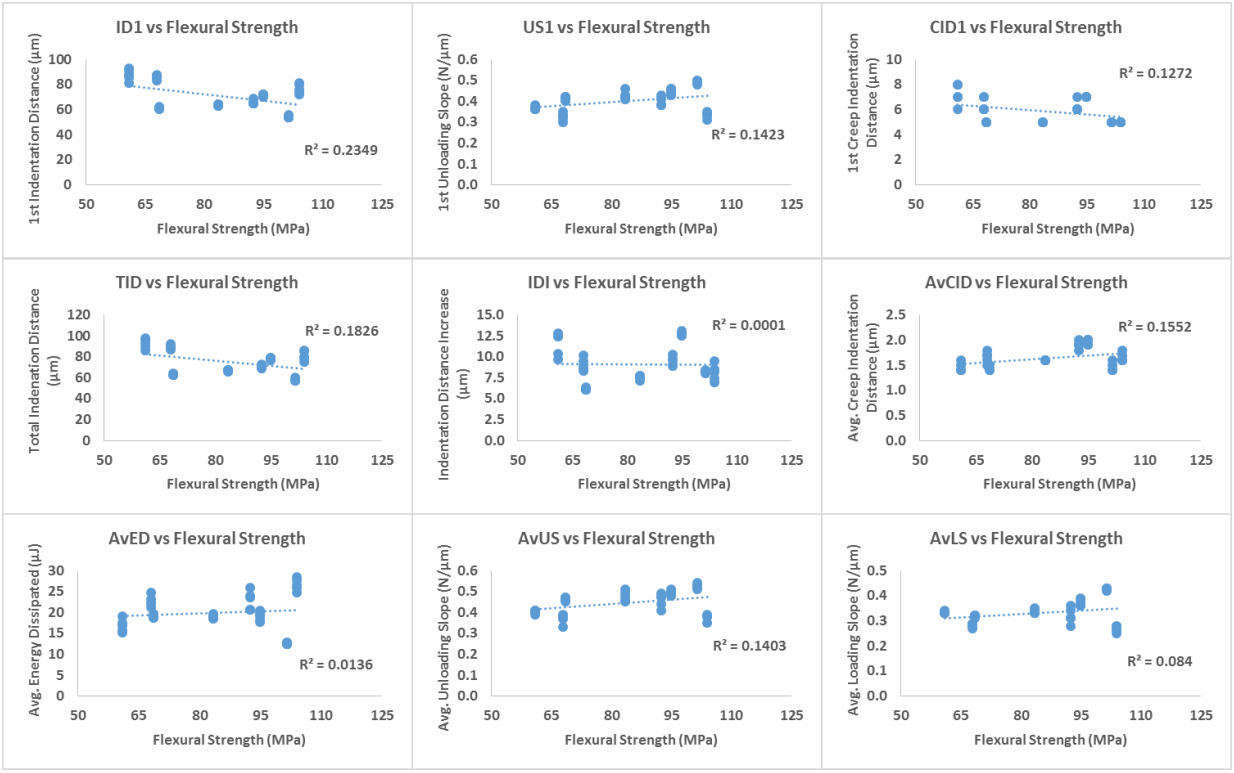

Figure 11: RPI outputs versus flexural strength.

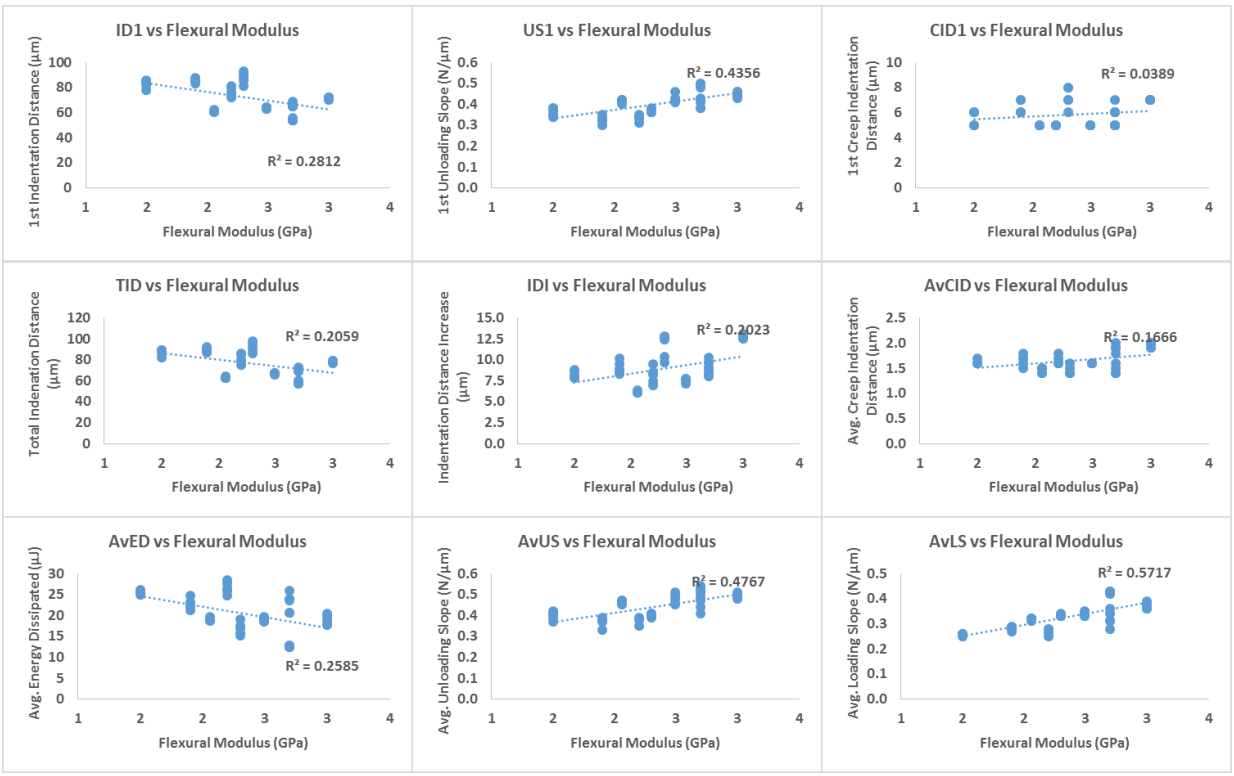

Figure 12: RPI outputs versus flexural modulus.

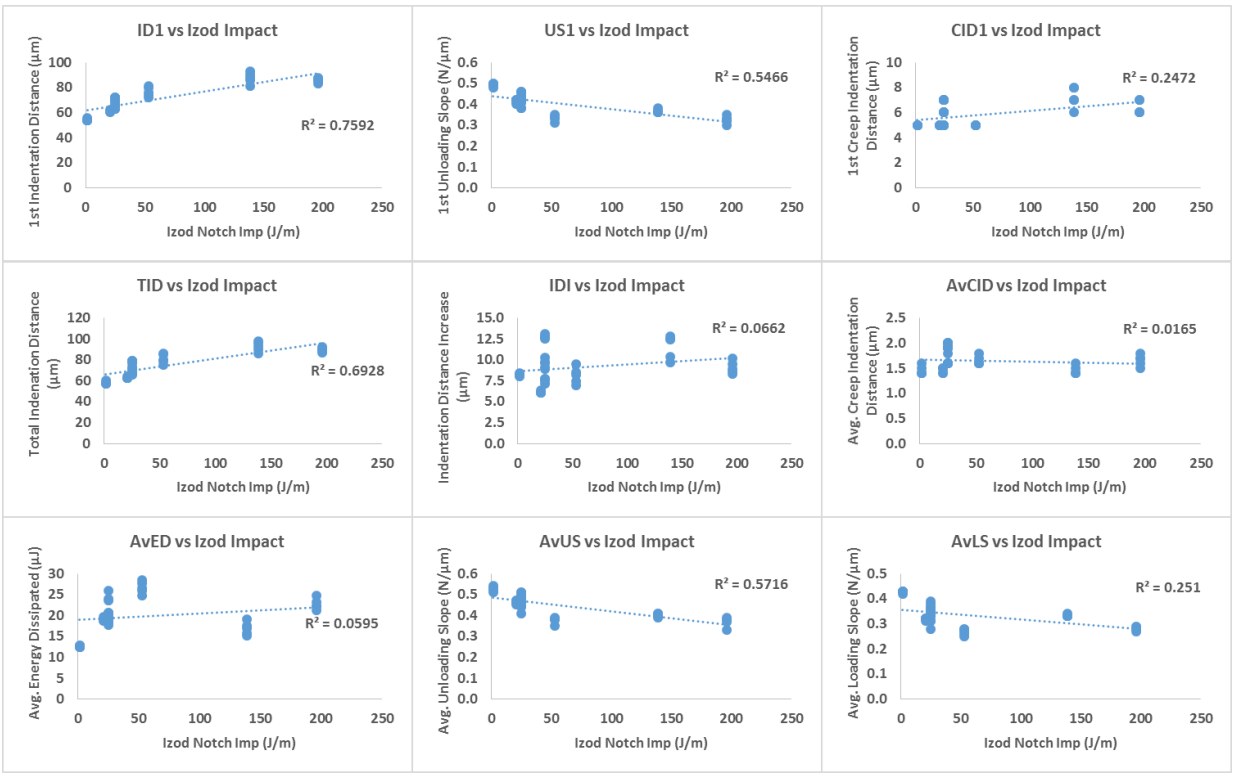

Figure 13: RPI outputs versus Izod notched impact energy.

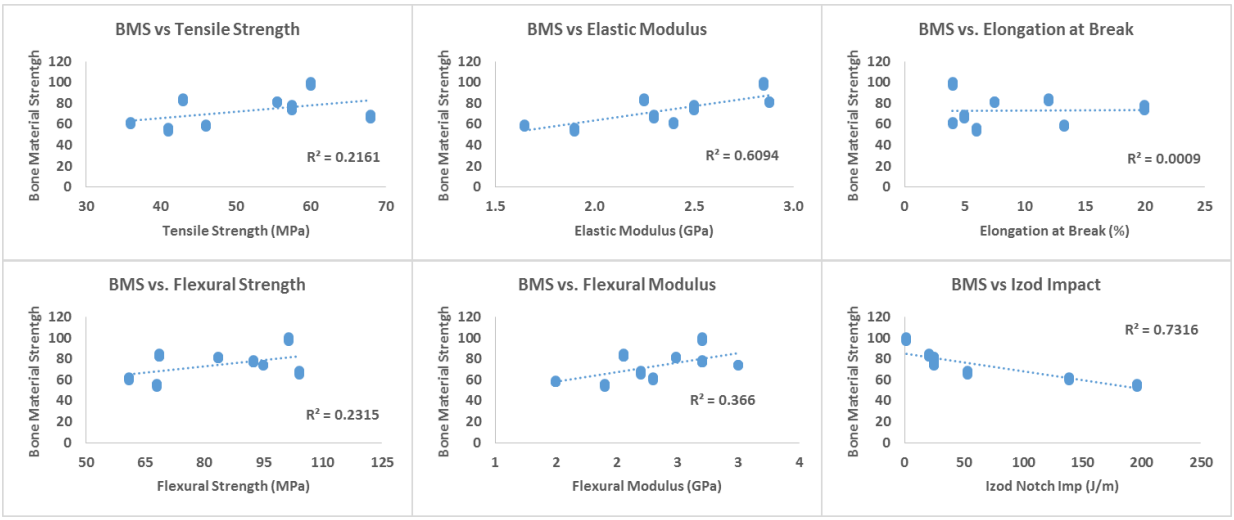

Figure 14: BMS versus mechanical properties.

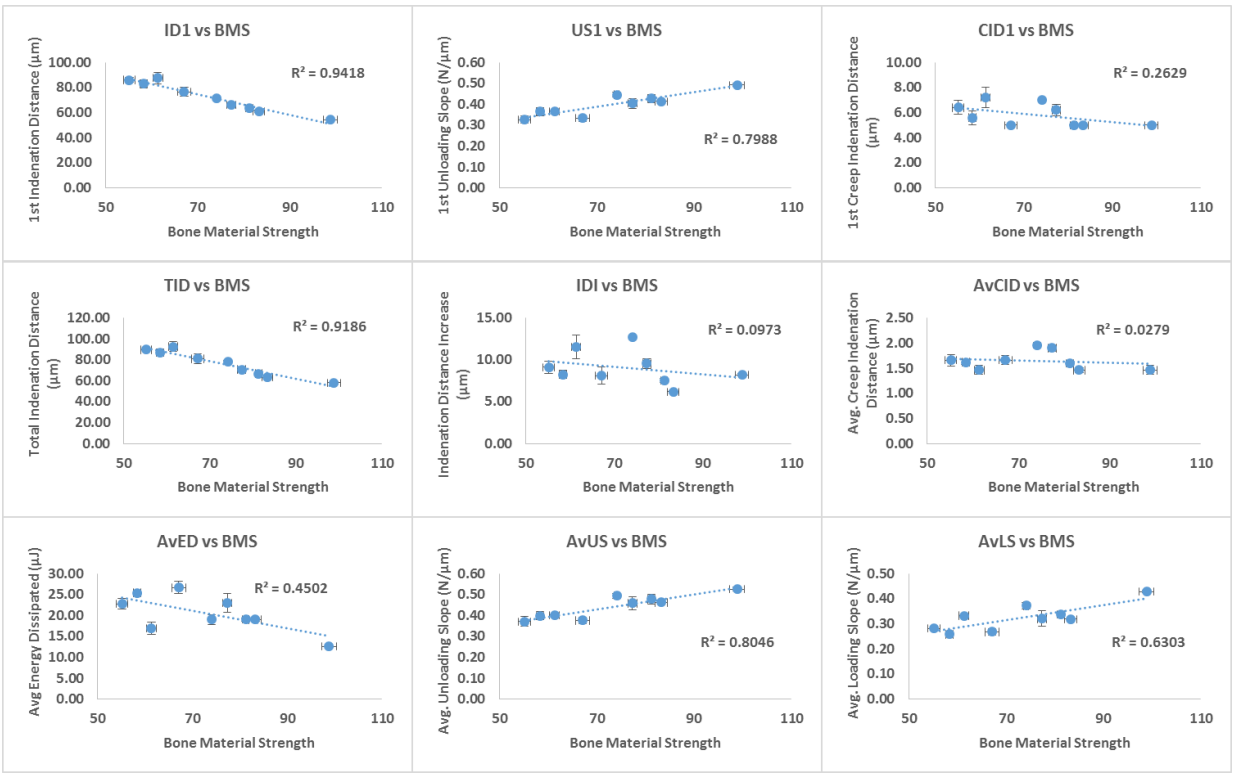

Figure 15: RPI outputs versus BMS.

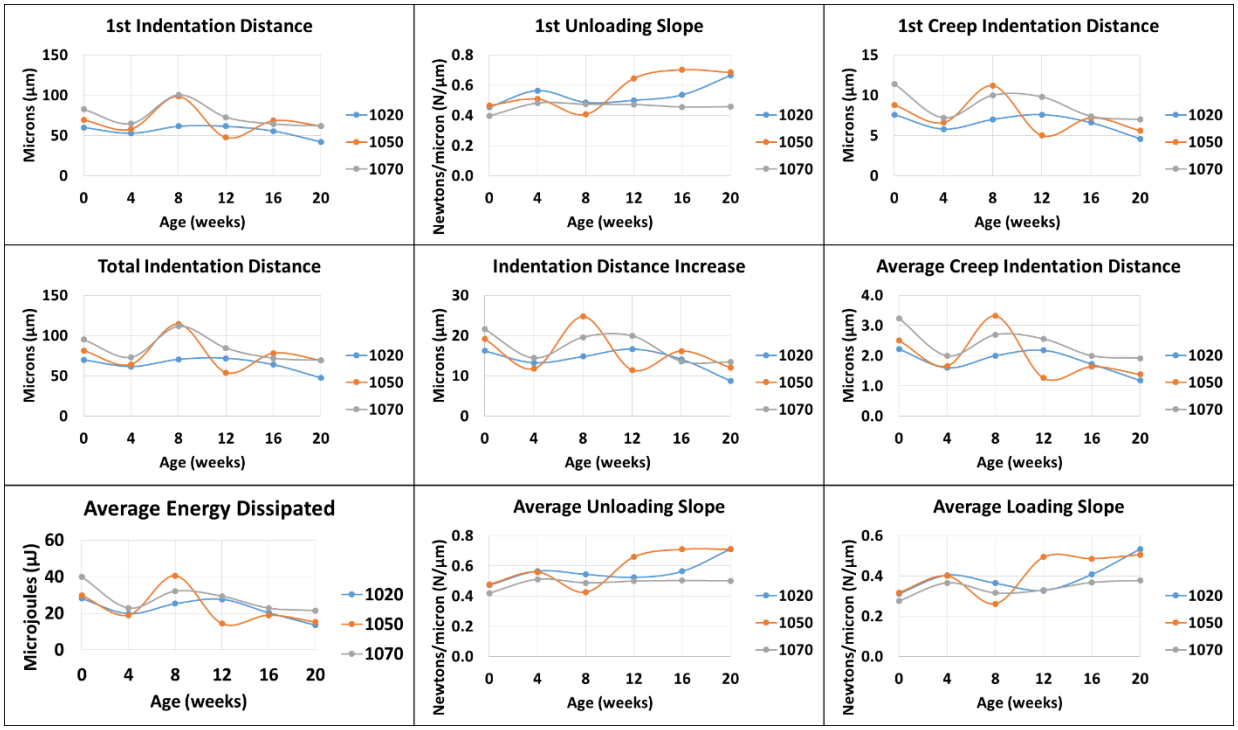

Figure 16: RPI outputs versus age for 6N force. 1020, 1050 and 1070 indicate the three separate genetic lines.

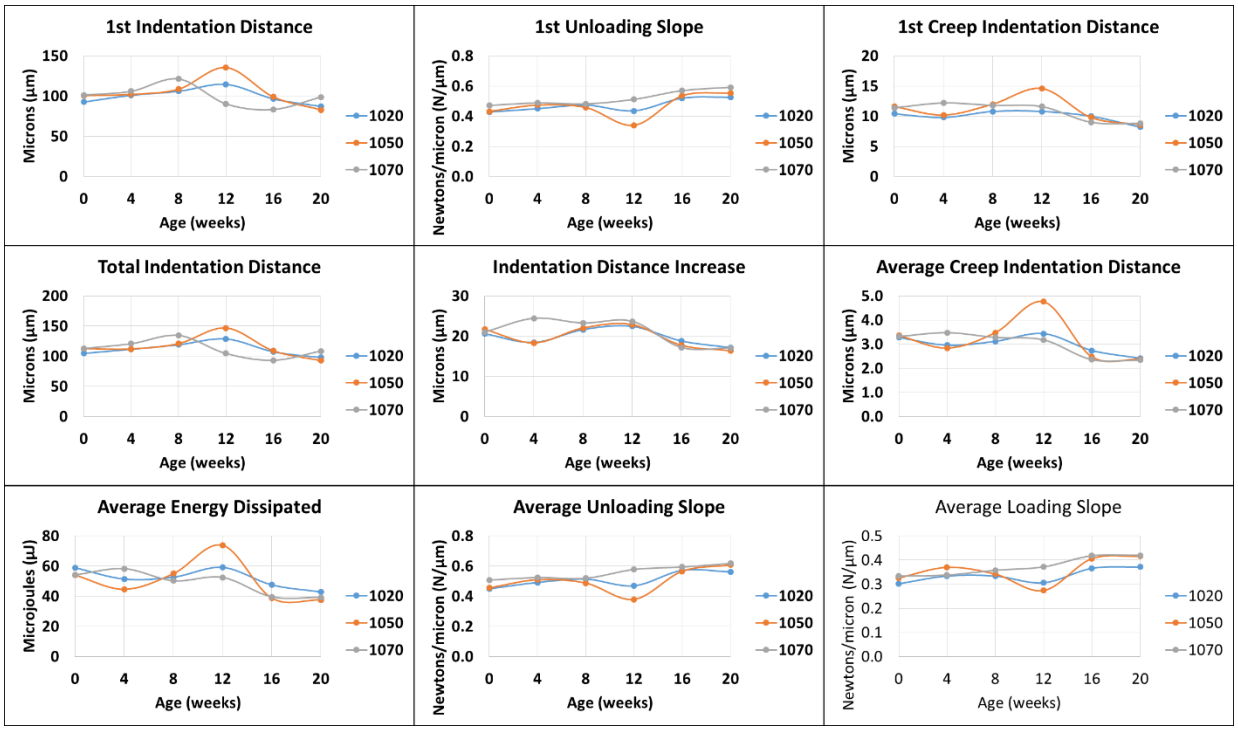

Figure 17: RPI outputs versus age for 8N force. 1020, 1050 and 1070 indicate the three separate genetic lines.

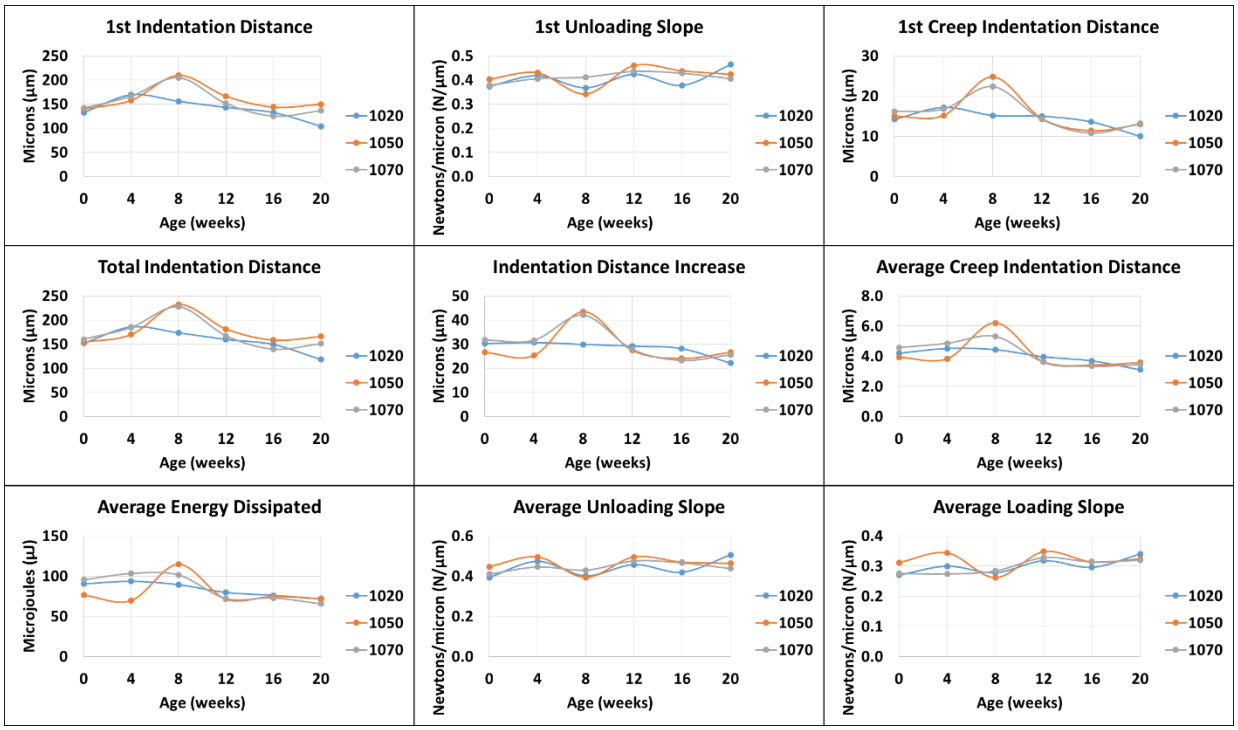

Figure 18: RPI outputs versus age for 10N force. 1020, 1050 and 1070 indicate the three separate genetic lines.

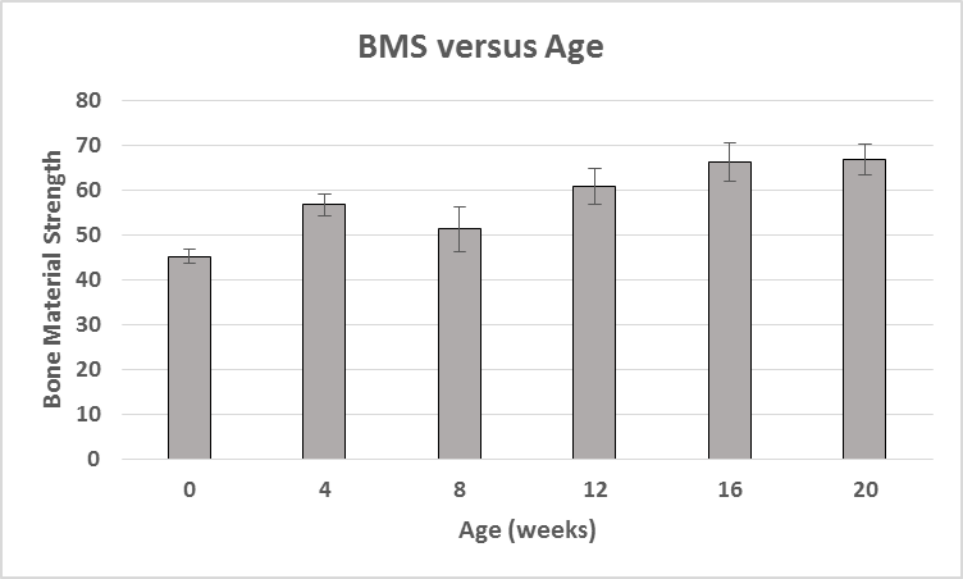

Figure 19: BMS versus age. Error bars indicate standard deviation.

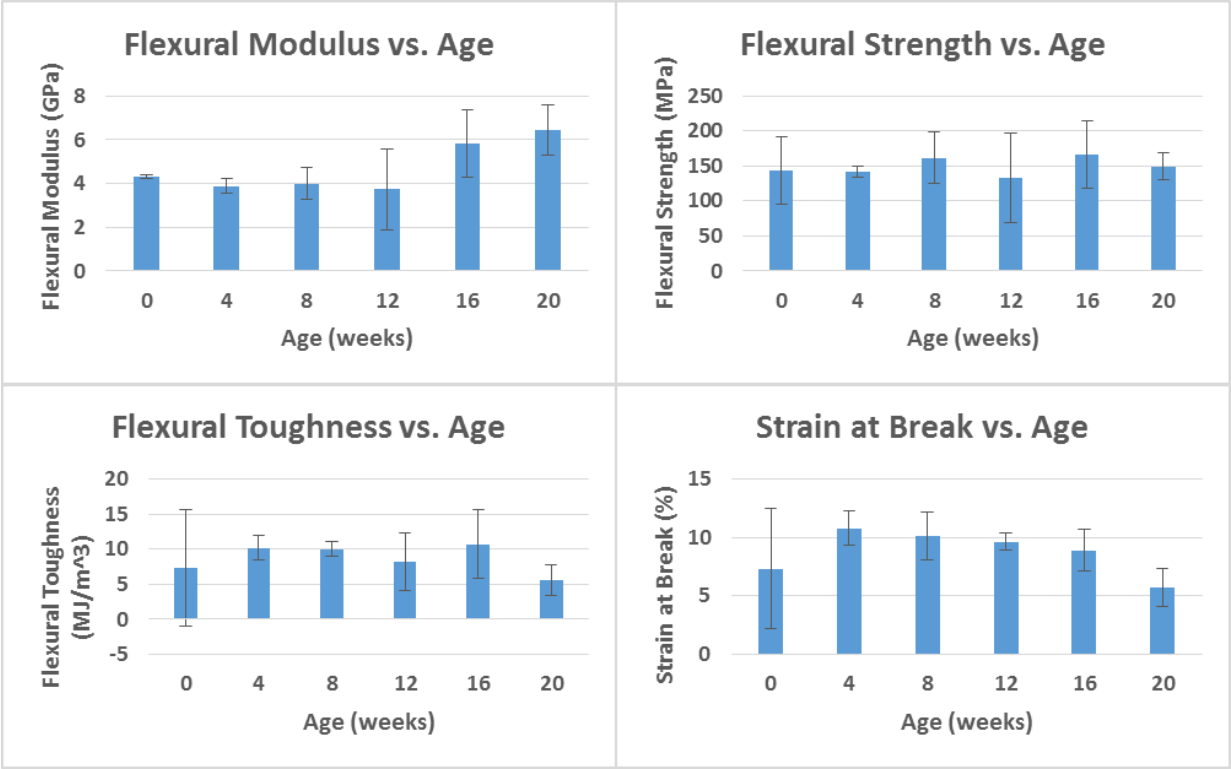

Figure 20: Three-point bend test calculated properties versus age. Error bars indicate standard deviation. The only significant differences ($p < 0.05$) exist between 20 weeks and 4, 8 and 12 weeks for flexural modulus and between 20 weeks and 4, 8, 12 and 16 weeks for strain at break.

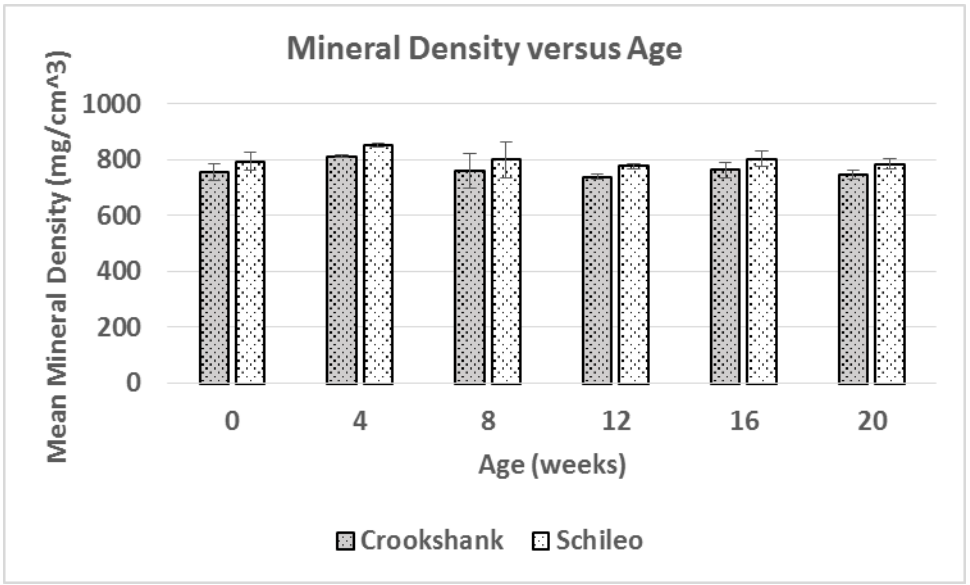

Figure 21: Mineral density calculated from HU obtained from CT scans versus age. Error bars indicate standard deviation.

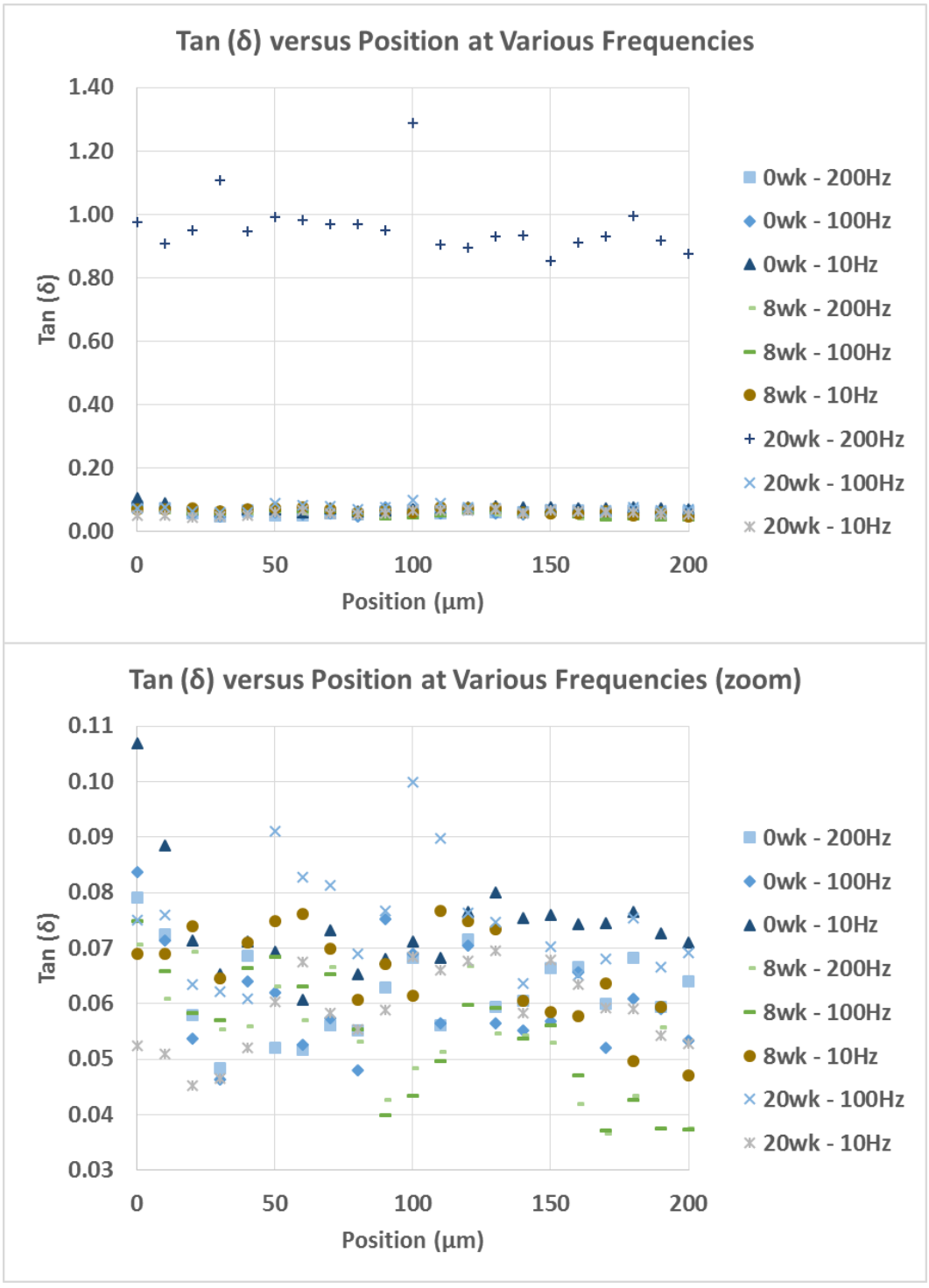

Figure 22: Tan (δ) versus position for select frequencies tested with dynamic nanoindentation. The second plot is a zoomed in view on the crowded data at the bottom of the first plot. Position measurements start at the outer edge of the sample.

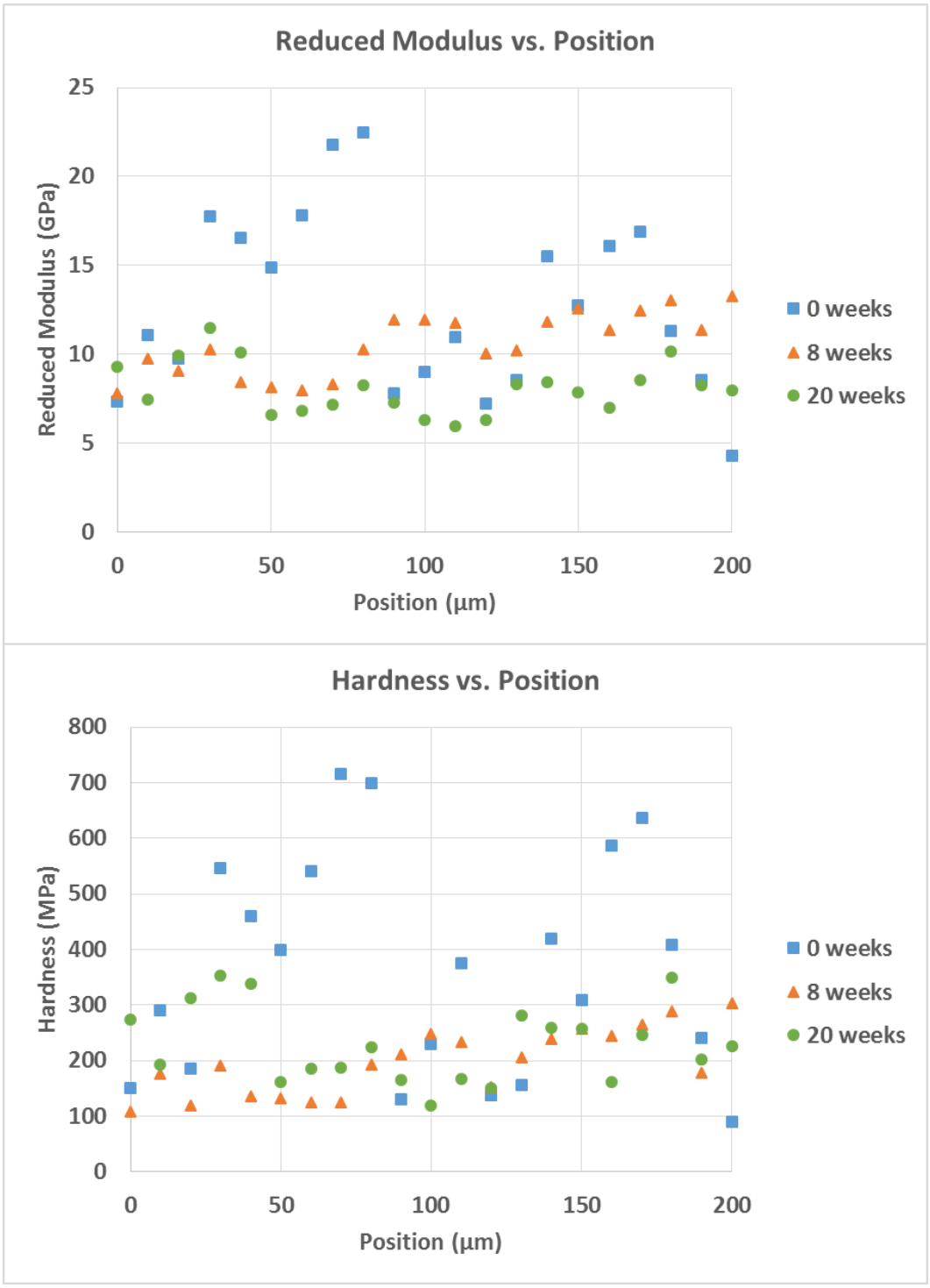

Figure 23: Reduced modulus and hardness versus age. Position measurements start at the outer edge of the sample.